Spin torques and charge transport on the surface of topological insulator

Akio Sakai and Hiroshi Kohno*

Division of Materials Physics, Department of Materials Engineering Science, Graduate School of Engineering Science, Osaka University, Toyonaka, Osaka 560-8531, Japan

(Received 1 March 2013; revised manuscript received 25 January 2014; published 14 April 2014)

We study various aspects of interplay between two-dimensional helical electrons, realized on the surface of a three-dimensional topological insulator, and the magnetization of a ferromagnet coupled to them. The magnetization is assumed to be perpendicular to the surface, with small transverse fluctuations $\boldsymbol{u}$. In the first part of this paper, we calculate spin torques that the helical electrons exert on the magnetization. Up to first orders with respect to $\boldsymbol{u}$, space/time derivative and electric current, we have determined all torques, which include Gilbert damping, spin renormalization, current-induced spin-orbit torques, and gradient corrections to them. Thanks to the identity between the velocity and spin in this model, these torques have exact interpretation in terms of transport phenomena, namely, diagonal conductivity, (anomalous) Hall conductivity, and corrections to them due to ordinary Hall effect on top of the anomalous one. These torque (and transport) coefficients are studied in detail with particular attention to the effects of vertex corrections and type of impurities (normal and magnetic). It is shown rigorously that the conventional current-induced torques, namely, spin-transfer torque and the so-called β term, are absent. An electromotive force generated by spin dynamics, which is the inverse to the current-induced spin-orbit torque, is also studied. In the second part, we study the feedback effects arising as combinations of current-induced spin-orbit torques and spin-dynamics-induced electromotive force. It is demonstrated that the Gilbert damping process in this system is completely understood as a feedback effect. Another feedback effect, which may be called "magnon-drag electrical conductivity," is shown to violate the exact correspondence between spin-torque and transport phenomena demonstrated in the first part.

DOI: 10.1103/PhysRevB.89.165307 PACS number(s): 73.43.−f, 72.25.Dc, 75.78.−n, 72.15.Gd

I. INTRODUCTION

Controlling a ferromagnetic moment by electric current has been studied extensively for more than a decade. This subject originates in a theoretical proposal of the spin-transfer effect [1,2], which is based on the conservation of spin angular momentum. Subsequently, it was noticed that there are dissipative [3,4] or nonadiabatic [5,6] corrections to the spin-transfer torque, which are not limited by the conservation law and thus may be utilized for more efficient control of magnetization. Recently, a new possibility was introduced which utilizes current-induced spin polarization due to spin-orbit coupling. Such "spin-orbit torques" can be expected in systems without inversion symmetry, most typically in systems with Rashba-type spin-orbit coupling [7–12]. Theoretical analysis of them, in particular including the spatial gradient of magnetization, is, however, quite complicated [13].

In a different branch of spintronics, a similar, but much simpler, system came into the real physical world. This is the surface states of a three-dimensional (3D) topological insulator [14,15]. In addition to its interest in itself [16–24], it may be regarded as an ideal system also in the context described in the previous paragraph since the kinetic energy consists purely of the Rashba term (hence takes a Dirac form). In fact, it is accessible by a clean physical [21,23] and analytical treatment, and sometimes allows exact statements. The purpose of this paper is to pursue an analytical treatment of this simple system, hopefully to gain some insight to study more complicated models such as the ordinary Rashba system. Another pleasant aspect of this simple model is that exact correspondences are expected among spin torque, charge transport, and electromotive force generated by magnetization dynamics.

A 3D topological insulator hosts on the surface a gapless two-dimensional (2D) Dirac electron system with ideally strong spin-orbit coupling. When coated with an insulating ferromagnet [25–27] or doped with magnetic impurities [28–30], a uniform and perpendicular component of magnetization opens a gap in the Dirac spectrum. The electron system in turn affects the magnetization, especially its dynamics, via spin torques. The current-induced "spin-orbit torques" in this system were first studied in the undoped case by Garate and Franz as a topological magnetoelectric effect with emphasis on its dissipationless nature [21]. Nomura and Nagaosa presented a new viewpoint on the electrical driving of domain wall based on their observation that a (Néel-type) domain wall is associated with electric charge (for the undoped case) [23]. Yokoyama *et al*. studied the doped case and found a much larger current-induced torque [22]. They also studied current-induced torques containing magnetization gradient, but with incorrect results [31]. Our principal aim in this paper is to further develop the theoretical study of spin torques. We determine all torques up to the first order in time derivative or spatial gradient, for a small-amplitude deviation of magnetization from the uniformly and perpendicularly magnetized state. The results on spin torques are readily translated into charge transport phenomena driven by an applied electric field or by an electromotive force generated by magnetization dynamics. We give a precise calculation of the linear-response coefficients describing these phenomena

*Present address: Department of Physics, Nagoya University, Furo-cho, Chikusa-ku, Nagoya 464-8601, Japan.

within the self-consistent Born approximation with ladder vertex corrections. Effects of magnetic impurities are also studied. The results found in this paper are summarized as follows:

(i) Spin torques with time derivative are exhausted by conventional ones, namely, Gilbert damping and spin renormalization. They are proportional to electrical conductivities (σ_{xx} and σ_{xy}) as noted before [22]. We show that this fact can be physically interpreted in terms of the feedback effect [see (iv) below].

(ii) Current-induced spin torques are exhausted by the so-called "spin-orbit torques" and gradient corrections to them. The conventional current-induced torques (spin-transfer torque and its dissipative correction called β term) are absent.

(iii) All torque coefficients can be (naively) related to transport coefficients. In particular, the absence of conventional current-induced torques can be understood as a consequence of gauge invariance in the transport picture.

(iv) The so-called feedback effects are discussed, which arise from the mutual coupling between spin dynamics and charge transport. In addition to feedback spin torques [32–35], we study a new type of feedback effect in which the charge transport is affected by the induced spin dynamics and the resulting electromotive force. The former gives Gilbert damping [35] and spin renormalization [see (i) above]. The latter appears as the modification of conductivity tensor and may be called "magnon-drag electrical conductivity."

(v) The correspondence between the torque coefficients and the transport coefficients, mentioned in (iii) above, breaks down if the feedback (or magnon-drag) effects are included in the transport coefficients.

(vi) The quantum anomalous Hall (QAH) state, realized when the chemical potential lies in the gap, is found to be fragile (not protected by the gap) in the following sense: low-frequency ac conductivity deviates from the QAH values (vanishing σ_{xx} and quantized σ_{xy}) by some powers of the frequency (at absolute zero temperature). This is due to the dynamical nature of the magnetization which causes the gap, and manifests as the feedback effect.

Through the calculation, we realized that the usual cutoff prescription (in terms of lattice constant, or Brillouin-zone size) to manage some divergent integrals fails to respect the Ward-Takahashi identity. This invalidates the gauge invariance and topological quantization of anomalous Hall conductivity. We are thus led to exploit another cutoff scheme and take the impurity-potential range as a cutoff which respects gauge invariance [36].

This paper is organized as follows. In Sec. II, we describe the model, Green's functions, and the regularization scheme to manage divergent integrals. Spin torques are calculated in Sec. III (Gilbert damping and spin renormalization) and Sec. IV (current-induced torques). The obtained results are discussed in terms of transport coefficients in Sec. V, and the feedback effects are studied in Sec. VI. Results and discussion are given in Sec. VII, and the summary is given in Sec. VIII. Calculational details are presented in the Appendices. Mathematical notations are summarized in the Supplemental Material [37]. Conceptually, this paper is divided into two parts: the first part (Secs. III–V) emphasizes the torque-transport correspondence, and the second part (Sec. VI) is related to its violation.

II. MODEL AND FORMULATION

A. Model

We consider a two-dimensional helical electron system coupled to a ferromagnetic moment by exchange interaction [17–20]. Such a system may be realized by depositing a ferromagnet [25–27] or by doping magnetic impurities which eventually order [28–30] on the surface of a topological insulator. In real materials, there are more or less deviations from the simple Dirac model, and also some complicating factors. For example, in the "magnetic coating" case, first-principles studies show the appearance of other (nontopological) band at the interface of most promising combination of realistic materials Bi_2Se_3/MnSe(111) [25,27]. In this paper, deferring the theoretical analysis of such complications to the future, or hoping for some experimental breakthroughs to reduce complications [38,39], we study a simple model Hamiltonian

$$\mathcal{H} = \sum_{\boldsymbol{k}} c_{\boldsymbol{k}}^{\dagger}[-\hbar v_{\mathrm{F}}(\boldsymbol{k}\times\boldsymbol{\sigma})^{z} - \mu]c_{\boldsymbol{k}} - M\int d\boldsymbol{r}\,(c^{\dagger}\boldsymbol{\sigma}c)_{\boldsymbol{r}}\cdot\boldsymbol{n}(\boldsymbol{r},t) + \hat{V}_{\mathrm{imp}}. \tag{1}$$

Here, $c^{\dagger} = (c_{\uparrow}^{\dagger}, c_{\downarrow}^{\dagger})$ and $c = {}^{t}(c_{\uparrow}, c_{\downarrow})$ are electron creation/annihilation operators, $\boldsymbol{\sigma}$ is a vector of Pauli matrices, and μ is the chemical potential. The first term represents kinetic energy with strong spin-orbit coupling of helical character. The second term is the exchange coupling to the ferromagnetic moment, whose spin direction is denoted by a unit vector $\boldsymbol{n}$, and M is a constant related to exchange splitting. The coupling to random impurities $\hat{V}_{\mathrm{imp}} = \int d\boldsymbol{r}\, c^{\dagger}(\boldsymbol{r})V_{\mathrm{imp}}(\boldsymbol{r})c(\boldsymbol{r})$ is detailed in the following. For the case of magnetic doping, the ferromagnetic order parameter will have spatial variation. The uniform part is expressed by M, and deviations from it may roughly be treated as magnetic impurities. We assume that the ferromagnetism is well developed and there is no sign change in the order parameter, and neglect any zero-mode effects [28,40].

For $M = 0$ (and $V_{\mathrm{imp}} = 0$), the electron dispersion $\varepsilon_{\boldsymbol{k}} = \pm\hbar v_{\mathrm{F}}k$ is gapless and linear in $k \equiv |\boldsymbol{k}|$. For $M \neq 0$ with a uniform magnetization $\boldsymbol{n} = \pm\hat{z}$, along the z direction, it acquires a gap as $\varepsilon_{\boldsymbol{k}} = \pm\sqrt{(\hbar v_{\mathrm{F}}k)^2 + M^2}$. This state supports a zero-field Hall conductivity $\sigma_{xy} \neq 0$, due to anomalous Hall effect, a combined effect of spin-orbit coupling and exchange splitting. When μ lies in the gap $|\mu| < |M|$, this system is in a quantum anomalous Hall (QAH) state and σ_{xy} takes a half-quantum value [41]

$$\sigma_{xy} = \frac{e^2}{2h}\,\mathrm{sgn}M_z \quad (|\mu| < |M|), \tag{2}$$

where $M_z = Mn_z = \pm M$, and $h = 2\pi\hbar$ is the Planck constant. Another peculiar feature of the model (1) is that the electron velocity

$$\boldsymbol{v} = v_{\mathrm{F}}(\hat{z}\times\boldsymbol{\sigma}) \tag{3}$$

is essentially given by spin [42]. This fact turns out to be useful for deeper understanding of the results.

As for impurities, we consider normal and magnetic impurities and take

$$V_{\rm imp}(\boldsymbol{r}) = \sum_i u(\boldsymbol{r}-\boldsymbol{R}_i) + \sum_j u_{\rm s}(\boldsymbol{r}-\boldsymbol{R}'_j)\boldsymbol{S}_j\cdot\boldsymbol{\sigma}, \quad (4)$$

where $\boldsymbol{S}_j$ represents the jth impurity spin. We focus on short-range potential and put $u(\boldsymbol{r}) \to u_0\delta(\boldsymbol{r})$ and $u_{\rm s}(\boldsymbol{r}) \to u_{\rm s}\delta(\boldsymbol{r})$ whenever possible (see Sec. II D). We take a Gaussian average over impurity positions as $\overline{V_{\rm imp}(\boldsymbol{r})V_{\rm imp}(\boldsymbol{r}')} = (n_{\rm i}u_0^2 + n_{\rm s}u_{\rm s}^2\overline{S_i^\alpha S_j^\beta}\sigma^\alpha\sigma^\beta)\delta(\boldsymbol{r}-\boldsymbol{r}')$, where $n_{\rm i}$ ($n_{\rm s}$) is the concentration of normal (magnetic) impurities. Averaging over impurity spin direction is taken as $\overline{S_i^\alpha} = 0$ and

$$\overline{S_i^\alpha S_j^\beta} = \delta_{ij}\delta^{\alpha\beta} \times \begin{cases} \overline{S_\perp^2} & (\alpha,\beta = x,y), \\ \overline{S_z^2} & (\alpha,\beta = z). \end{cases} \quad (5)$$

In the main text, we consider only the normal impurities for simplicity (except for figures). Modifications due to magnetic impurities are summarized in Appendix A 4. Throughout, we assume weak impurity scattering.

B. Spin torque

Dynamics of the ferromagnetic moment, or spin $\boldsymbol{n}$, is described by the Landau-Lifshitz-Gilbert (LLG) equation

$$\dot{\boldsymbol{n}} = \gamma_d \boldsymbol{H}_{\rm eff}\times\boldsymbol{n} - \alpha_d\,\boldsymbol{n}\times\dot{\boldsymbol{n}} + \boldsymbol{t}'. \quad (6)$$

Putting aside the ordinary precessional and damping torques (first and second terms, with effective field $\gamma_d\boldsymbol{H}_{\rm eff}$ and damping constant α_d coming from all but conduction electrons), the effects of conduction electrons are contained in the third term. It comes from the exchange interaction $-M\boldsymbol{n}\cdot\hat{\boldsymbol{\sigma}}$, where $\hat{\boldsymbol{\sigma}} = c^\dagger\boldsymbol{\sigma}c$, and is given by

$$\boldsymbol{t} = M\boldsymbol{n}\times\langle\hat{\boldsymbol{\sigma}}\rangle \equiv s_0\boldsymbol{t}'. \quad (7)$$

The second equality in Eq. (7) defines $\boldsymbol{t}'$ in Eq. (6), where

$$s_0 = \hbar S/a^2 \quad (8)$$

is the angular-momentum density of the ferromagnetic moment, with a^2 being the area on the surface per localized spin S which carries the ferromagnetic moment.

In systems with weak spin-orbit coupling (with inversion symmetry), spin torques are generally expected to have the form [3,4]

$$\boldsymbol{t}' = -\alpha_c\,(\boldsymbol{n}\times\dot{\boldsymbol{n}}) - \frac{\delta S}{S}\,\dot{\boldsymbol{n}} - \left(\boldsymbol{v}_{\rm s}^0\cdot\nabla\right)\boldsymbol{n} - \beta\,\boldsymbol{n}\times\left(\boldsymbol{v}_{\rm s}^0\cdot\nabla\right)\boldsymbol{n} \quad (9)$$

in the first order in time derivative and spatial gradient of $\boldsymbol{n}$. The first term is the Gilbert damping with damping constant α_c. The second term contributes to renormalize the spin from S to

$$S_{\rm tot} = S + \delta S \quad (10)$$

by including the electron spin δS. These lead to

$$\alpha = (\alpha_d + \alpha_c)\frac{S}{S+\delta S} \quad (11)$$

as the total damping constant [43]. The third term is the spin-transfer torque, with $\boldsymbol{v}_{\rm s}^0$ being a velocity proportional to spin-current density, and the fourth term is its dissipative correction due to spin-relaxation processes [3,44–46], called the β term [4]. Other types of torques can be expected in the presence of nonadiabaticity [5,6] or spin-orbit coupling (in systems with broken inversion symmetry) [7,8].

In this paper, we restrict ourselves to a small-amplitude magnetization dynamics around a uniformly magnetized state $\boldsymbol{n} = \pm\hat{z}$ and write as [44,45]

$$\boldsymbol{n} = \pm\hat{z}\sqrt{1-\boldsymbol{u}^2} + \boldsymbol{u} \simeq \pm\hat{z} + \boldsymbol{u}, \quad (12)$$

where $\boldsymbol{u}(\boldsymbol{r},t) = (u^x,u^y,0)$ is a small transverse component. By calculating the spin density in the first order in $\boldsymbol{u}$, we obtain spin torques from Eq. (7). It is convenient to divide the Hamiltonian as $\mathcal{H} = \mathcal{H}_0 + \mathcal{H}_1$:

$$\mathcal{H}_0 = \sum_{\boldsymbol{k}} c_{\boldsymbol{k}}^\dagger\left[-\hbar v_{\rm F}(\boldsymbol{k}\times\boldsymbol{\sigma})^z - M_z\sigma^z - \mu\right]c_{\boldsymbol{k}} + \hat{V}_{\rm imp}, \quad (13)$$

$$\mathcal{H}_1 = -M\int d\boldsymbol{r}\,(c^\dagger\boldsymbol{\sigma}c)_{\boldsymbol{r}}\cdot\boldsymbol{u}(\boldsymbol{r},t), \quad (14)$$

where

$$M_z = Mn_z = \pm M. \quad (15)$$

In the first order in $\mathcal{H}_1$, hence in $\boldsymbol{u}$, the electron spin acquires a transverse component $\langle\hat{\boldsymbol{\sigma}}_\perp\rangle \perp \hat{z}$ and contributes to the spin torque

$$\boldsymbol{t} = M_z\hat{z}\times\langle\hat{\boldsymbol{\sigma}}_\perp\rangle. \quad (16)$$

We focus on torques up to the first order in $\boldsymbol{u}$.

Some remarks are in order. For the case of magnetic coating, the spin torques act at the interface whereas the ferromagnet has a finite thickness, hence $\boldsymbol{t}'$ in Eq. (6) should be divided by the number of atomic layers of the ferromagnet [22].

For the case of magnetic doping, it is possible that the magnetization is entirely carried by helical electrons ("itinerant ferromagnetism"). In this case, one may wonder whether the expressions for the torque such as Eqs. (7) and (16) make sense since both $\boldsymbol{n}$ and $\boldsymbol{\sigma}$ come from the same electrons. However, careful studies show that the appropriate results can be obtained from the present results by simply setting $S = 0$ while keeping the conduction electron components (such as δS) [45,46].

C. Green's function

The (retarded) Green's function for $\mathcal{H}_0$ is given by

$$G_{\boldsymbol{k}}^{\rm R}(\varepsilon) = \left[\varepsilon + \hbar v_{\rm F}(\boldsymbol{k}\times\boldsymbol{\sigma})^z + M_z\sigma^z + \mu - \hat{\Sigma}(\boldsymbol{k},\varepsilon)\right]^{-1} \equiv (g_0 + \boldsymbol{g}\cdot\boldsymbol{\sigma})D_{\boldsymbol{k}}^{\rm R}(\varepsilon), \quad (17)$$

where $\hat{\Sigma} = \Sigma_0 + \boldsymbol{\Sigma}\cdot\boldsymbol{\sigma}$ with $\boldsymbol{\Sigma} = (\Sigma_1,\Sigma_2,\Sigma_3)$ is the (retarded) self-energy due to impurity scattering, and

$$g_0(\varepsilon) = \varepsilon + \mu - \Sigma_0(\varepsilon), \quad (18)$$

$$\boldsymbol{g}(\varepsilon) = -\hbar v_{\rm F}(\hat{z}\times\boldsymbol{k}) - M_z\hat{z} + \boldsymbol{\Sigma}(\boldsymbol{k},\varepsilon), \quad (19)$$

$$D_{\boldsymbol{k}}^{\rm R}(\varepsilon) = [(g_0)^2 - (\boldsymbol{g})^2]^{-1}. \quad (20)$$

As described in the next section, Σ_0 and Σ_3 depend only on ε but not on $\boldsymbol{k}$, whereas Σ_1 and Σ_2 depend only on $\boldsymbol{k}$ (and not

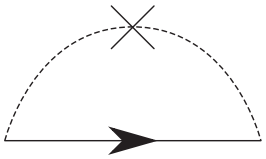

FIG. 1. Self-energy in the Born approximation.

on ε). At $\varepsilon = 0$, Σ_0 and Σ_3 can be taken to be pure imaginary

$$\Sigma_0(0) = -i\gamma, \quad \Sigma_3(0) = -i\gamma' \tag{21}$$

by neglecting the real parts. (The real parts can be absorbed into the definition of μ and M_z [47].) The damping constants γ and γ' are calculated in the first Born approximation (Fig. 1) as [48]

$$\gamma = \gamma_0 |\mu| \Theta(\mu^2 - M^2), \quad \gamma' = -(M_z/\mu)\gamma, \tag{22}$$

where $\Theta(x)$ is the Heaviside step function, $\Theta(x < 0) = 0$, $\Theta(x > 0) = 1$, and the dimensionless parameter

$$\gamma_0 = \frac{n_{\rm i} u_0^2}{4(\hbar v_{\rm F})^2} \tag{23}$$

is assumed to be small (compared to unity). As for $\hat{\Sigma}_\perp \equiv \Sigma_1\sigma^x + \Sigma_2\sigma^y$, it is calculated as (see below) [36]

$$\hat{\Sigma}_\perp(\boldsymbol{k}) = \frac{\gamma_0}{\pi + \gamma_0} \hbar v_{\rm F}(\boldsymbol{k} \times \boldsymbol{\sigma})^z. \tag{24}$$

The Green's function is thus written as

$$\hat{G}^{\rm R}_{\boldsymbol{k}}(\varepsilon) = [\,\varepsilon + \mu + \hbar\tilde{v}_{\rm F}(\boldsymbol{k} \times \boldsymbol{\sigma})^z + M_z\sigma^z - \hat{\Sigma}_\parallel(\varepsilon)]^{-1}, \tag{25}$$

where $\hat{\Sigma}_\parallel = \Sigma_0 + \Sigma_3\sigma^z$, and

$$\tilde{v}_{\rm F} = \frac{\pi}{\pi + \gamma_0} v_{\rm F} \equiv \xi v_{\rm F} \tag{26}$$

is the renormalized velocity with

$$\xi = \frac{\pi}{\pi + \gamma_0} \tag{27}$$

being the renormalization constant. In the following calculation, the full ε dependence of Σ_0 and Σ_3 is necessary at the intermediate stage (when there is a "Fermi-sea term"), but the final results depend only on those at $\varepsilon = 0$.

D. Regularization

In the calculation, we encounter divergent integrals such as $\sum_{\boldsymbol{k}} D_{\boldsymbol{k}}$, and some consistent procedure is needed to handle them. Usually, a momentum cutoff $\Lambda_{\rm BZ}$ is introduced to limit the single-particle states to $|\boldsymbol{k}| < \Lambda_{\rm BZ}$ [49]. However, this is not favorable from the viewpoint of theoretical consistency such as gauge invariance and topological quantization (see Appendix A 5). In fact, the Ward-Takahashi identity [50]

$$v_i + \frac{1}{\hbar}\frac{\partial \hat{\Sigma}(\boldsymbol{k},\varepsilon)}{\partial k_i} = \tilde{\Lambda}_i(\boldsymbol{k},\varepsilon) \tag{28}$$

between the self-energy $\hat{\Sigma}(\boldsymbol{k},\varepsilon)$ and the current vertex function $\tilde{\Lambda}_i(\boldsymbol{k},\varepsilon)$ does not hold since the δ-function potential leads to a $\boldsymbol{k}$-independent self-energy but the vertex function is nonvanishing

$$\tilde{\Lambda}_i(\boldsymbol{k},\varepsilon) = \frac{\pi}{\pi + \gamma_0} v_{\rm F}(\hat{z} \times \boldsymbol{\sigma})_i, \tag{29}$$

as deduced from Eqs. (A56) or (A66) in Appendix A.

As a systematic method to overcome this unpleasant situation, we introduce a (short-distance) cutoff in the range of the impurity potential, and smear the δ-function potential. Deferring the details to elsewhere [36], we summarize the results as follows. The self-energy is determined in the self-consistent Born approximation by

$$\hat{\Sigma}(\boldsymbol{k},\varepsilon) = n_{\rm i} \sum_{\boldsymbol{k}'} |u_{\boldsymbol{k}-\boldsymbol{k}'}|^2 G^{\rm R}_{\boldsymbol{k}'}(\varepsilon), \tag{30}$$

where $u_{\boldsymbol{k}}$ is the Fourier component of the impurity potential whose range is finite (not zero like a δ function). The self-energy then acquires a $\boldsymbol{k}$ dependence, and the result is given by Eq. (24). The Ward-Takahashi identity (28) is thus satisfied. The total self-energy is given by $\hat{\Sigma} = \hat{\Sigma}_\parallel + \hat{\Sigma}_\perp$, where $\hat{\Sigma}_\parallel(\varepsilon) \equiv \Sigma_0(\varepsilon) + \Sigma_3(\varepsilon)\sigma^z$ is determined from the self-consistent equations

$$\Sigma_0(\varepsilon) = n_{\rm i} u_0^2 [\varepsilon + \mu - \Sigma_0(\varepsilon)] \sum_{|\boldsymbol{k}| < \Lambda_{\rm imp}} D_{\boldsymbol{k}}(\varepsilon), \tag{31}$$

$$\Sigma_3(\varepsilon) = -n_{\rm i} u_0^2 [M_z - \Sigma_3(\varepsilon)] \sum_{|\boldsymbol{k}| < \Lambda_{\rm imp}} D_{\boldsymbol{k}}(\varepsilon), \tag{32}$$

where we have chosen $u_{\boldsymbol{k}} = u_0\Theta(\Lambda_{\rm imp} - |\boldsymbol{k}|)$ with $\Lambda_{\rm imp}$ being the potential-range cutoff. Equations (31) and (32) are formally the same as those obtained based on the ordinary cutoff [51] $\Lambda_{\rm BZ}$, but there is a crucial difference in $\hat{\Sigma}_\perp$. In this paper, we use the self-consistent equations (31) and (32) to remove the divergence encountered in the calculation [see Eq. (B15)]. After removing the divergences, we evaluate the resulting expressions based on the first Born approximation (for the self-energy).

III. GILBERT DAMPING AND SPIN RENORMALIZATION

Gilbert damping constant α_c and spin renormalization δS, both due to conduction electrons, can be read from the ω-linear terms of the transverse spin susceptibility [52] $\chi_\perp^{\alpha\beta}(\omega) = \langle\langle\, \hat{\sigma}_\perp^\alpha; \hat{\sigma}_\perp^\beta \rangle\rangle_{\omega+i0}(\alpha,\beta = x,y)$ as [45]

$$\lim_{\omega\to 0} \frac{\chi_\perp^{\alpha\beta}(\omega) - \chi_\perp^{\alpha\beta}(0)}{i\omega} = \frac{s_0}{M^2}\left\{\alpha_c\delta_\perp^{\alpha\beta} \pm \frac{\delta S}{S}\varepsilon^{\alpha\beta}\right\}, \tag{33}$$

where $\delta_\perp^{\alpha\beta} = \delta^{\alpha\beta} - \delta^{\alpha z}\delta^{\beta z}$, and $\pm$ corresponds to $n_z = \pm 1$ [see Eq. (12)]. This is derived by considering the linear response of the electron spin density $\langle\hat{\sigma}_\perp^\alpha(\boldsymbol{0})\rangle_\omega = M\chi_\perp^{\alpha\beta}(\omega)u^\beta(\omega)$ to a time-dependent (but uniform) magnetization $\boldsymbol{n}(t) = \pm\hat{z} + \boldsymbol{u}(\omega)\,e^{-i\omega t}$ (the perturbation is $\mathcal{H}_1$) and using Eq. (16). The form of Eq. (33), which has been confirmed by the present explicit calculation, shows that torques which are first order in $\dot{\boldsymbol{u}}$ are exhausted by [53]

$$\boldsymbol{t}_1' = \mp\alpha_c(\hat{z} \times \dot{\boldsymbol{u}}) - \frac{\delta S}{S}\dot{\boldsymbol{u}}. \tag{34}$$

This fact turns out to be crucial in the discussion in Sec. VI.

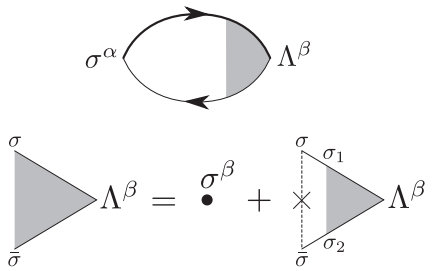

FIG. 2. Feynman diagram for transverse spin susceptibility (upper diagram). Λ^β represents the renormalized vertex defined by the lower diagrams.

For convenience, we introduce $\tilde{\alpha}$ and $\delta\tilde{S}$ by

$$\alpha_c = (a/\lambda_M)^2\,\tilde{\alpha}/S, \quad \delta S = (a/\lambda_M)^2\,\delta\tilde{S}, \tag{35}$$

where

$$\lambda_M = 2\pi\hbar v_{\rm F}/|M| \tag{36}$$

is the "Compton wavelength" for a particle with mass $|M|/v_{\rm F}^2$ and for a "light velocity" $v_{\rm F}$. (This is defined by using the bare velocity.) With [54,55] $v_{\rm F} = 4\times10^5$ m/s and $a = 0.5$ nm, we may estimate as $\lambda_M \sim 17$ nm, $(a/\lambda_M)^2 \sim 10^{-3}$ for $M = 0.1$ eV, and $\lambda_M \sim 170$ nm, $(a/\lambda_M)^2 \sim 10^{-5}$ for $M = 0.01$ eV.

The diagrammatic expression for $\chi_\perp^{\alpha\beta}(i\omega_\lambda) \equiv \langle\langle\,\hat{\sigma}^\alpha;\hat{\sigma}^\beta\,\rangle\rangle_{i\omega_\lambda}$ is shown in Fig. 2. Let us first consider the contribution without vertex corrections

$$\chi_\perp^{\alpha\beta}(i\omega_\lambda) = -T\sum_n\sum_{\boldsymbol{k}}{\rm tr}[\sigma^\alpha G_{\boldsymbol{k}}^+\sigma^\beta G_{\boldsymbol{k}}]. \tag{37}$$

Here and hereafter, we express the dependence on the Matsubara frequency as $G^+ = G(i\varepsilon_n + i\omega_\lambda)$, $G = G(i\varepsilon_n)$. We defer the details of calculation to Appendix A 1, but note here that $\tilde{\alpha}$ and $\delta\tilde{S}$ (without vertex corrections) generally consist of three terms

$$\tilde{\alpha} = \tilde{\alpha}' + \tilde{\alpha}'' + \tilde{\alpha}''', \tag{38}$$

$$\delta\tilde{S} = \delta\tilde{S}' + \delta\tilde{S}'' + \delta\tilde{S}'''. \tag{39}$$

Here, $\mathcal{O}'$, $\mathcal{O}''$, and $\mathcal{O}'''$ (with $\mathcal{O} = \tilde{\alpha},\delta\tilde{S}$) refer to the first, second, and third terms, respectively, in Eqs. (A11) and (A12). These are characterized as follows: $\mathcal{O}'$ comes from the analytic continuation $(G^+,G) \to (G^{\rm R},G^{\rm A})$, and $\mathcal{O}''$ and $\mathcal{O}'''$ come from $(G^+,G) \to (G^{\rm R},G^{\rm R})$ or $(G^{\rm A},G^{\rm A})$. Often, $\mathcal{O}'$ and $\mathcal{O}''$ are called Fermi-surface terms, and $\mathcal{O}'''$ a Fermi-sea term.

The results are given as follows. For the "doped" case $|\mu| > |M|$, where the chemical potential μ lies in the band, we obtain

$$\tilde{\alpha}' = \frac{\pi}{2}\frac{1+\gamma_0^2}{\gamma_0}\frac{\mu^2-M^2}{\mu^2+M^2}(1-\chi_\zeta), \tag{40}$$

$$\tilde{\alpha}'' = 1, \tag{41}$$

$$\delta\tilde{S}' = \frac{2\pi M|\mu|}{\mu^2+M^2}(1-\chi_\zeta), \tag{42}$$

$$\delta\tilde{S}''' = \tan^{-1}\left[\frac{2\gamma_0}{1-\gamma_0^2}\frac{2M|\mu|}{\mu^2-M^2}\right], \tag{43}$$

and $\tilde{\alpha}''' = \delta\tilde{S}'' = 0$, where

$$\chi_\zeta = \frac{1}{\pi}\tan^{-1}\left[\frac{2\gamma_0}{1-\gamma_0^2}\frac{\mu^2+M^2}{\mu^2-M^2}\right], \tag{44}$$

with $0 \leqslant \chi_\zeta \leqslant \frac{1}{2}$. The results without vertex corrections are given by $\tilde{\alpha} = \tilde{\alpha}' + \tilde{\alpha}''$ and $\delta\tilde{S} = \delta\tilde{S}' + \delta\tilde{S}'''$.

The vertex corrections are taken into account by replacing the bare vertex σ^β by the renormalized vertex Λ^β. This is described in Appendix A 3. The results (with velocity renormalization) are given by [53]

$$\tilde{\alpha} = \xi^{-2}\rho\,(\tilde{\alpha}'\cos\theta \mp \delta\tilde{S}'\sin\theta) + \xi^{-1}\tilde{\alpha}'', \tag{45}$$

$$\delta\tilde{S} = \xi^{-2}\rho\,(\delta\tilde{S}'\cos\theta \pm \tilde{\alpha}'\sin\theta) + \delta\tilde{S}''', \tag{46}$$

which amounts to rotation (by θ) and dilation (by ρ or ξ) in spin space. The θ, ρ, and ξ are given in Appendix A 3. Explicitly, we have

$$\tilde{\alpha} = \frac{\pi}{\gamma_0}\frac{(1-\chi_\zeta)(\mu^2-M^2)}{(1+\chi_\zeta)\mu^2+(3-\chi_\zeta)M^2}, \tag{47}$$

$$\delta\tilde{S} = \frac{8\pi(1-\chi_\zeta)(\mu^2+M^2)M|\mu|}{[(1+\chi_\zeta)\mu^2+(3-\chi_\zeta)M^2]^2} + \tan^{-1}\left(\gamma_0\frac{4M|\mu|}{\mu^2-M^2}\right), \tag{48}$$

where we have deliberately neglected γ_0 and γ_0^2 compared to unity. If $|\mu|$ is not close to $|M|$, χ_ζ and $\tan^{-1}(\ldots)$ are of order γ_0, and have

$$\tilde{\alpha} = \frac{\pi}{\gamma_0}\frac{\mu^2-M^2}{\mu^2+3M^2}, \tag{49}$$

$$\delta\tilde{S} = 8\pi M|\mu|\frac{\mu^2+M^2}{(\mu^2+3M^2)^2}, \tag{50}$$

which coincide with the previous works (on transport coefficients) [56,57].

For the "undoped" case, namely, when μ lies in the gap $|\mu| < |M|$, we have

$$\tilde{\alpha} = 0, \tag{51}$$

$$\delta\tilde{S} = \pi\,{\rm sgn}M, \tag{52}$$

irrespective of whether the vertex corrections are included or not. [When the vertex corrections are included, the velocity renormalization is also taken into account. This assures the Ward-Takahashi identity (28) and the "half-quantum" value of $\delta\tilde{S}$ [58].]

These results are plotted in Figs. 3 and 4 as functions of μ. In both figures, the curve 1 contains RA-type and RR-type vertex corrections as well as the velocity renormalization (ρ,θ, and ξ plotted in Fig. 5) [59]. The curve 2 includes no vertex corrections ($\theta = 0$, $\rho = \xi = 1$). Note that the magnitude of the actual parameters is obtained by multiplying a small factor $(a/\lambda_M)^2$ [see Eq. (35)].

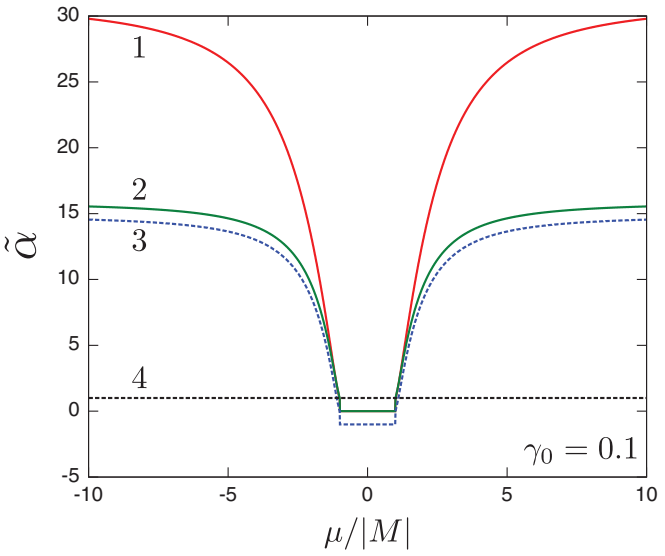

FIG. 3. (Color online) Normalized Gilbert damping constant $\tilde{\alpha}$ [Eq. (35)] as a function of chemical potential μ for $\gamma_0 = 0.1$, with (1) and without (2) vertex corrections. Partial contributions $\tilde{\alpha}'$ and $\tilde{\alpha}''$ are also plotted as 3 and 4, respectively.

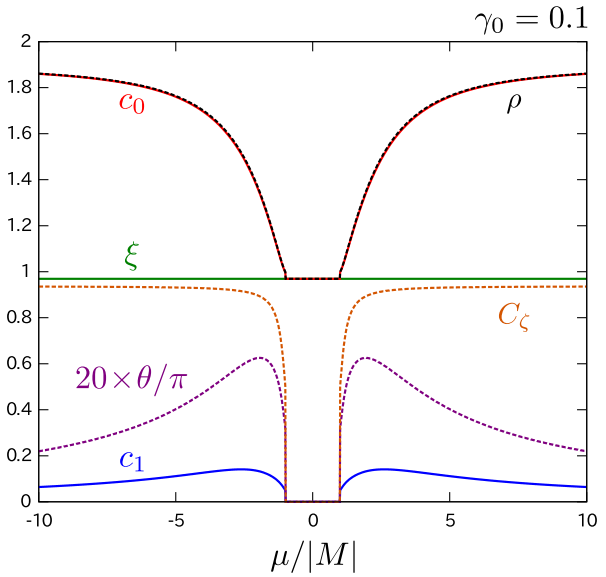

FIG. 5. (Color online) Parameters c_0, c_1, ρ, θ [see Eqs. (A59)–(A61)], ξ and C_ζ [see Eq. (B12)] as functions of μ for $\gamma_0 = 0.1$. c_0 and ρ are almost overlapped.

One sees from the figures that both $\tilde{\alpha}$ and $\delta\tilde{S}$ are enhanced by the vertex corrections. As will be discussed in Sec. V, these quantities are equivalent to electrical conductivities σ_{xx} and σ_{xy}, respectively. The enhancement is then naturally understood as due to the dominance of forward scattering in the impurity scattering. Namely, spin-conserving scattering is dominated by forward scattering for $|\mu| \gg |M|$ because of the "spin-momentum locking" on the Fermi surface. [Note that the electron spin sees the vector Re $\boldsymbol{g}$, Eq. (19), as an effective magnetic field.] This feature is weakened for $|\mu| \lesssim 2|M|$ and diminishes as μ approaches the band edge because of finite $g_3 \sim -M$.

For δS, even a qualitative feature is changed from a monotonically decreasing behavior (without vertex corrections) to a peaked one (with vertex corrections) as a function of $|\mu|$. This is mainly due to the mixing of $\tilde{\alpha}'$ which is much larger than $\delta\tilde{S}'$ for $|\mu| > |M|$. This mixing is allowed because of the violation of time-reversal symmetry (and parity) by M.

The effects of vertex corrections are expected to change if we include magnetic impurities which cause spin-flip scattering. Examples are shown in Figs. 6 and 7 for $\tilde{\alpha}$ and

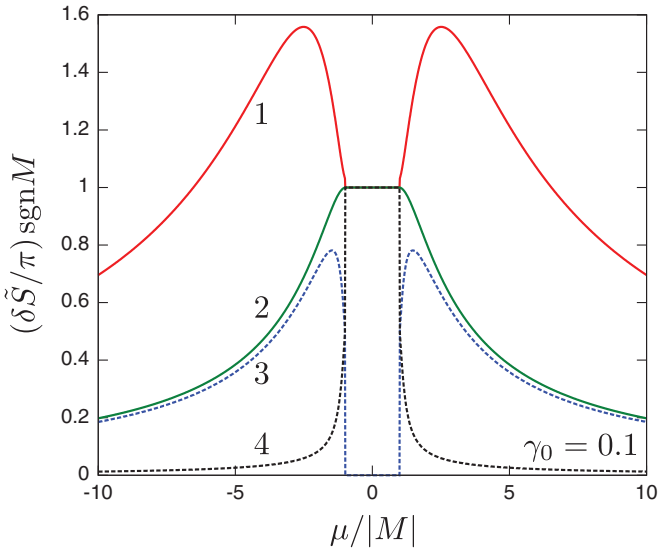

FIG. 4. (Color online) Normalized spin renormalization $\delta\tilde{S}$ [Eq. (35)] as a function of chemical potential μ for $\gamma_0 = 0.1$, with (1) and without (2) vertex corrections. Partial contributions $\delta\tilde{S}'$ and $\delta\tilde{S}'''$ are also plotted as 3 and 4, respectively.

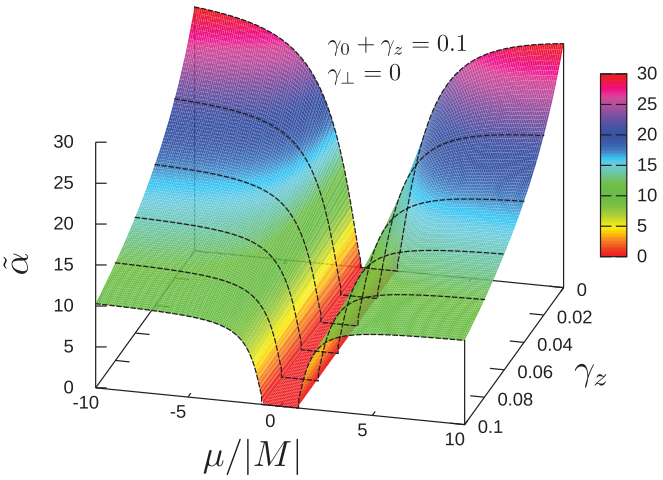

FIG. 6. (Color online) Normalized Gilbert damping constant $\tilde{\alpha}$ as a function of chemical potential μ in the presence of magnetic impurities (γ_z) in addition to normal impurities (γ_0). Their relative magnitudes are changed by keeping $\gamma_0 + \gamma_z = 0.1$ and $\gamma_\perp = 0$. See Eq. (A76) for the notations.

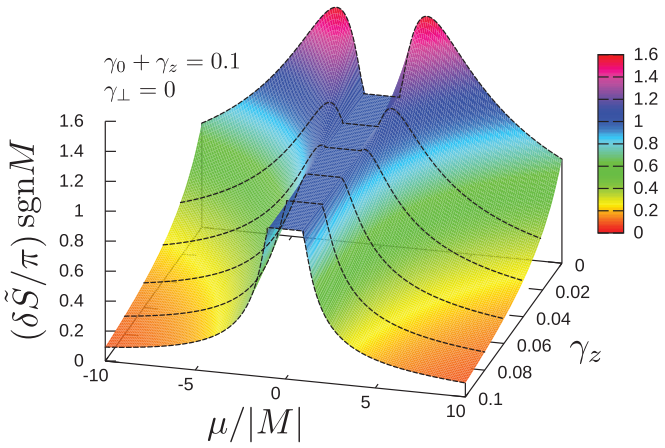

FIG. 7. (Color online) Normalized spin renormalization $\delta\tilde{S}$ as a function of chemical potential μ in the presence of magnetic impurities (γ_z) in addition to normal impurities (γ_0). Their relative magnitudes are changed by keeping $\gamma_0+\gamma_z=0.1$ and $\gamma_\perp=0$.

$\delta\tilde{S}$, respectively, for the case of "Ising-type" impurity spins which point to the normal to the surface of a topological insulator. As the magnetic (spin-flip) scattering, quantified by its contribution γ_z to the electron damping [see Eq. (A75) for the definition], is increased relative to the spin-conserving scattering (γ_0), the effect of vertex corrections changes from the enhancement (for $\gamma_z<\gamma_0$) to suppression (for $\gamma_z>\gamma_0$). The curves at $\gamma_z=\gamma_0$ exactly coincide with those without vertex corrections (curves 2 in Figs. 3 and 4). The results (not shown) for "XY-type" impurity spins, which point to the in-plane direction, show similar behavior but with a more moderate dependence on the corresponding damping parameter ($\gamma_\perp$). The difference comes from the difference in the spin-flip rate.

The fact that the sign of δS is the same as the sign of M is quite natural in view of the fact that $S+\delta S$ enters the LLG equation as the total spin (angular momentum). Namely, the spin of the conduction electrons (δS) will be parallel to the d spin (S) if $M>0$, and anti-parallel if $M<0$. However, it should be distinguished from the equilibrium spin polarization $\langle\hat{\sigma}^z\rangle_0$ since δS is a dynamical quantity (obtained as an ω-linear term in the response function), and does not necessarily coincide with $\langle\hat{\sigma}^z\rangle_0$ when there are spin-nonconserving processes [3] such as due to the spin-orbit coupling [60].

The value of δS in the limit $\mu,M\to 0$ depends on the way the limit is taken; if $\mu\to 0$ is taken first, we have $\delta\tilde{S}\to\pi\,\mathrm{sgn}M$, whereas if $M\to 0$ is taken first, we have $\delta\tilde{S}\to 0$. In the former case, δS is discontinuous at $M=0$. This is known as "parity anomaly" in field theory [61].

It is worth noting that, when μ lies in the gap, $\delta\tilde{S}'''$ has a topological character and takes a quantized value $\delta\tilde{S}'''=\pi\,\mathrm{sgn}M$, as shown in Appendix A 5. We stress that such a topological argument remains valid in the presence of impurities (or self-energy in general) if the Ward-Takahashi identity (28), or $\partial G/\partial(\hbar k_i)=G\tilde{\Lambda}_iG$, is satisfied [58]. This requires a careful treatment of ultraviolet divergence in the calculation of self-energy as mentioned in Sec. II D.

IV. CURRENT-INDUCED TORQUES

For current-induced torques, we consider a static but spatially varying magnetization $\boldsymbol{n}(\boldsymbol{r})=\pm\hat{z}+\boldsymbol{u}(\boldsymbol{q})\,e^{i\boldsymbol{q}\cdot\boldsymbol{r}}$ and calculate electrons' spin polarization $\langle\hat{\sigma}^\alpha_\perp\rangle$ in a state with an Ohmic current. We introduce an external electric field $\boldsymbol{E}$ to drive a current, and apply the linear-response theory to this perturbation:

$$\langle\hat{\sigma}^\alpha_\perp\rangle=\lim_{\omega\to 0}\frac{K^\alpha_i(\boldsymbol{q},\omega+i0)-K^\alpha_i(\boldsymbol{q},0)}{i\omega}E_i, \tag{53}$$

where [52] $K^\alpha_i(\boldsymbol{q},i\omega_\lambda)=\langle\!\langle\,\hat{\sigma}^\alpha_\perp(\boldsymbol{q});\hat{J}_i\,\rangle\!\rangle_{i\omega_\lambda}$ describes the response of $\hat{\sigma}^\alpha$ to $\boldsymbol{E}$ which perturbs the total electric current $\hat{\boldsymbol{J}}=-e\sum_{\boldsymbol{k}\sigma}c^\dagger_{\boldsymbol{k}\sigma}\boldsymbol{v}c_{\boldsymbol{k}\sigma}$. We look at the spin density whose wave vector $\boldsymbol{q}$ comes from the magnetization texture.

As noted by Garate and Franz [21], the response (53) is already finite in a state with uniform magnetization $\boldsymbol{n}=\pm\hat{z}$. Thanks to the spin-velocity equivalence (3), and as will be discussed in Sec. V, we readily obtain the spin density [53]

$$\langle\boldsymbol{\sigma}_\perp\rangle=\frac{e}{4\pi^2\hbar v_{\mathrm{F}}}\{\pm\delta\tilde{S}\,\boldsymbol{E}+\tilde{\alpha}\,(\hat{z}\times\boldsymbol{E})\}, \tag{54}$$

or the torque density [53]

$$\boldsymbol{t}_2=\frac{eM}{4\pi^2\hbar v_{\mathrm{F}}}\{\,\delta\tilde{S}\,(\hat{z}\times\boldsymbol{E})\mp\tilde{\alpha}\boldsymbol{E}\}. \tag{55}$$

The coefficients ($\delta\tilde{S}$ and $\tilde{\alpha}$) are precisely the same as those calculated in the previous section. Garate and Franz [21] considered the case $|\mu|<|M|$, where only the $\delta\tilde{S}$ term is present. Yokoyama *et al.* [22] pointed out that the $\tilde{\alpha}$ term is also present (and much larger than $\delta\tilde{S}$) for the doped case $|\mu|>|M|$. Here, we see that they are enhanced by vertex corrections (Figs. 3 and 4) if the effects of magnetic impurities are not too strong.

In this paper, we proceed further and calculate torques in the first order in $\boldsymbol{u}$ (and $\boldsymbol{q}$). By expanding K^α_i with respect to $\boldsymbol{u}$ (namely, $\mathcal{H}_1$) and $\boldsymbol{q}$ both in the first order, we write

$$K^\alpha_i(\boldsymbol{q},i\omega_\lambda)=-eMK^{\alpha\beta}_{ij}(i\omega_\lambda)\,q_ju^\beta(\boldsymbol{q}). \tag{56}$$

The coefficient $K^{\alpha\beta}_{ij}$ is expressed diagrammatically in Fig. 8. For example, the contribution without vertex corrections [Fig. 8(a)] is given by

$$K^{\alpha\beta}_{ij}(i\omega_\lambda)=T\sum_n\sum_{\boldsymbol{k}}\{\mathrm{tr}[\sigma^\alpha(\partial_jG^+_{\boldsymbol{k}})\sigma^\beta G^+_{\boldsymbol{k}}v_iG_{\boldsymbol{k}}] -\mathrm{tr}[\sigma^\alpha G^+_{\boldsymbol{k}}v_iG_{\boldsymbol{k}}\sigma^\beta(\partial_jG_{\boldsymbol{k}})]\}. \tag{57}$$

This is calculated in Appendix A 2, and the result is

$$K^{\alpha\beta}_{ij}(\omega+i0)=\frac{\omega}{M^2}\,(A\,\varepsilon^{i\alpha}+B\,\delta^{i\alpha}_\perp)\,\delta^{\beta j}_\perp+\mathcal{O}(\omega^2), \tag{58}$$

where A and B are dimensionless coefficients presented below. The torque density is thus obtained as

$$\boldsymbol{t}_3=e\,\{-A\boldsymbol{E}+B\,(\hat{z}\times\boldsymbol{E})\}\,\mathrm{div}\boldsymbol{u}, \tag{59}$$

where $\mathrm{div}\boldsymbol{u}=(\partial u_x/\partial x)+(\partial u_y/\partial y)$. Inclusion of vertex corrections shown in Fig. 8(b) does not change the functional form of the torque, but modifies the coefficients A and B (see below). These are calculated in Appendix A 3. Contributions with another type of vertex corrections shown in Fig. 8(c) turn out to vanish [62].

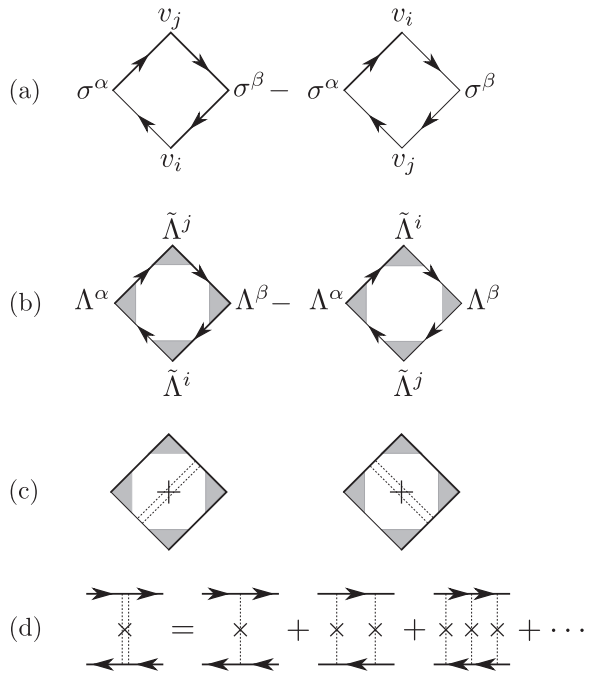

FIG. 8. Diagrammatic expression for $K_{ij}^{\alpha\beta}$ without (a) and with (b), (c) vertex corrections. The shaded triangles in (b) and (c) represent renormalized vertices: the one with Λ^α represents a renormalized spin (σ^α) vertex, and that with $\tilde{\Lambda}_i$ represents a renormalized velocity (v_i) vertex. The former has been defined in Fig. 2(b), and the latter is defined by $\tilde{\Lambda}_i = -v_F \varepsilon_{i\alpha} \Lambda^\alpha$. The double line with a cross in (c) represents a ladder defined in (d).

Note the peculiar combination $\mathrm{div}\boldsymbol{u} = \boldsymbol{\nabla}\cdot\boldsymbol{u}$, of $\boldsymbol{\nabla}$ and $\boldsymbol{u}$ in Eq. (59), which is different from the spin-transfer torque and the β term [see Eq. (9)]; while the (vectorial) direction of the spin-transfer torque (and the β term) is determined by the spin direction $\boldsymbol{u}$, the direction of the present torque [Eq. (59)] is determined by $\boldsymbol{E}$, and we see that the latter is just the gradient correction to Eq. (55). Since the present calculation shows that all torques of the form $E_i \partial_j u^\beta$ are exhausted by Eq. (59), we conclude that the spin-transfer torque and the β term are absent in the present system. This fact will be reinforced by the gauge-invariance argument in Sec. V.

The coefficients A and B are given by Eqs. (A48)–(A51), or more explicitly as follows. For $|\mu| > |M|$, we have obtained

$$A' = -\frac{1}{2\pi^2}\frac{\mu M^2 M_z}{\mu^2 + M^2}\,\Psi, \tag{60}$$

$$B' = \frac{M^2}{8\pi^2}\frac{1+\gamma_0^2}{\gamma_0}\frac{\mu^2 - M^2}{\mu^2 + M^2}\,\Psi\,\mathrm{sgn}\mu, \tag{61}$$

$$B''' = \frac{\gamma_0}{3\pi^2}\frac{M^2(\mu^2 + M^2)}{W_0}\,\mathrm{sgn}\mu, \tag{62}$$

and $A'' = A''' = B'' = 0$, with

$$\Psi = \frac{(\mu^2 - M^2)\left(1-\gamma_0^2\right)}{W_0} + \frac{\pi(1-\chi_\zeta)}{2\gamma_0(\mu^2 + M^2)}, \tag{63}$$

$$W_0 = \left(1-\gamma_0^2\right)^2(\mu^2 - M^2)^2 + (2\gamma_0)^2(\mu^2 + M^2)^2$$
$$\simeq (\mu^2 - M^2)^2 + (2\gamma_0)^2(\mu^2 + M^2)^2. \tag{64}$$

Here, we have used $\gamma = \gamma_0|\mu|$, and ρ, θ, and χ_ζ are given as before. [It is legitimate to neglect γ_0^2 compared to unity, as done in Eq. (64), also in B' and Ψ.] The results without vertex corrections are given by $A = A'$ and $B = B' + B'''$. If the vertex corrections are included, we have

$$A = \rho^2\,(A'\cos 2\theta - B'\sin 2\theta), \tag{65}$$

$$B = \rho^2\,(B'\cos 2\theta + A'\sin 2\theta) + \xi^2 B''', \tag{66}$$

or

$$A = -\frac{2}{\pi}\mu M^2 M_z\left(\frac{\mu^4 - M^4}{\pi W_0} + \frac{1-\chi_\zeta}{2\gamma_0}\right)\frac{(3-\chi_\zeta)\mu^2 + (1+\chi_\zeta)M^2}{[(1+\chi_\zeta)\mu^2 + (3-\chi_\zeta)M^2]^3}, \tag{67}$$

$$B = \left\{\frac{1}{2\pi\gamma_0}\left(\frac{\mu^4 - M^4}{\pi W_0} + \frac{1-\chi_\zeta}{2\gamma_0}\right)\frac{\mu^2 - M^2}{[(1+\chi_\zeta)\mu^2 + (3-\chi_\zeta)M^2]^2} + \frac{\gamma_0}{3(\pi+\gamma_0)^2}\frac{\mu^2 + M^2}{W_0}\right\}M^2\,\mathrm{sgn}\mu. \tag{68}$$

If $|\mu|$ is not close to $|M|$, these can be approximated as

$$A = -\frac{1}{4\pi\gamma_0}\frac{M^2 M_z \mu}{(\mu^2 + M^2)^2}, \tag{69}$$

$$B = \frac{1}{16\pi\gamma_0^2}\frac{(\mu^2 - M^2)M^2}{(\mu^2 + M^2)^2}\,\mathrm{sgn}\mu \tag{70}$$

for the case without vertex corrections, and

$$A = -\frac{1}{\pi\gamma_0}\frac{(3\mu^2 + M^2)M^2 M_z \mu}{(\mu^2 + 3M^2)^3}, \tag{71}$$

$$B = \frac{1}{4\pi\gamma_0^2}\frac{(\mu^2 - M^2)M^2}{(\mu^2 + 3M^2)^2}\,\mathrm{sgn}\mu \tag{72}$$

for the case with vertex corrections. For small γ_0, the coefficients grow as $A \propto \gamma_0^{-1}$ and $B \propto \gamma_0^{-2}$.

For $|\mu| < |M|$, we have

$$A = B = 0, \tag{73}$$

irrespective of whether the vertex corrections are included or not. This means that the torques in Eq. (55) get no corrections due to magnetization gradient. In particular, $\delta\tilde{S}$ is not affected by the inhomogeneity of magnetization, and this fact reinforces the topological nature of $\delta\tilde{S}$ in the QAH state.

The coefficients A and B are plotted in Fig. 9 as functions of μ. Both quantities are enhanced by the vertex corrections for spin-conserving impurity scattering. Inclusion of magnetic impurities tends to suppress them, as shown in Fig. 10.

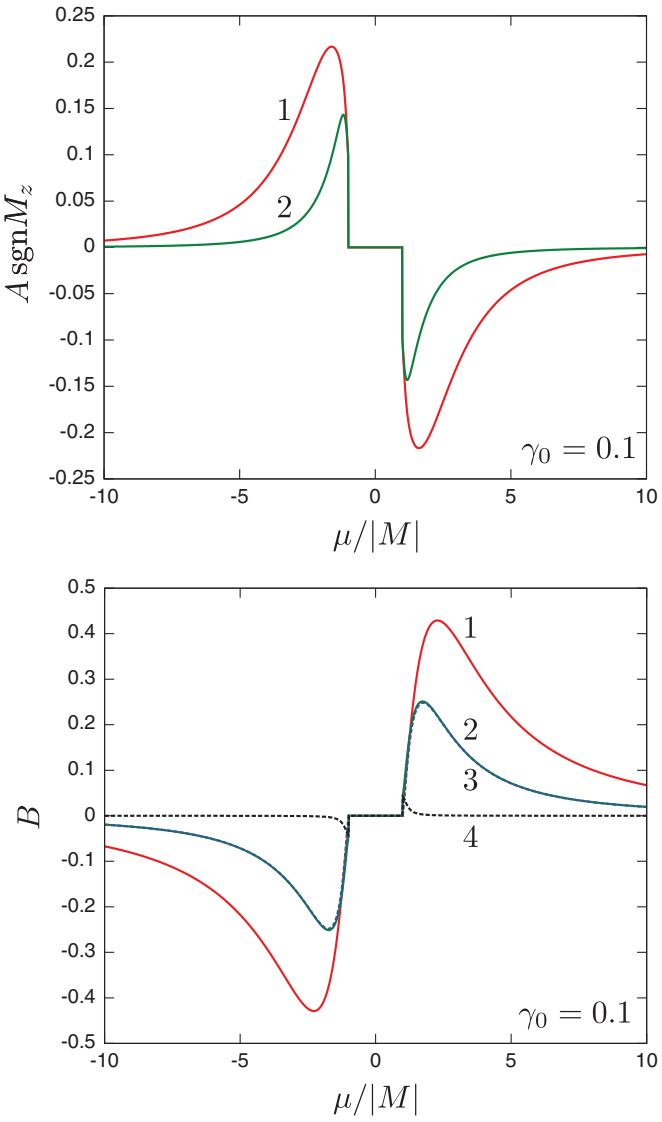

FIG. 9. (Color online) The coefficients A and B of current-induced torques with magnetization gradient as functions of chemical potential μ for $\gamma_0 = 0.1$, with (1) and without (2) vertex corrections. For B, partial contributions B' and B''' are also plotted as 3 and 4, respectively.

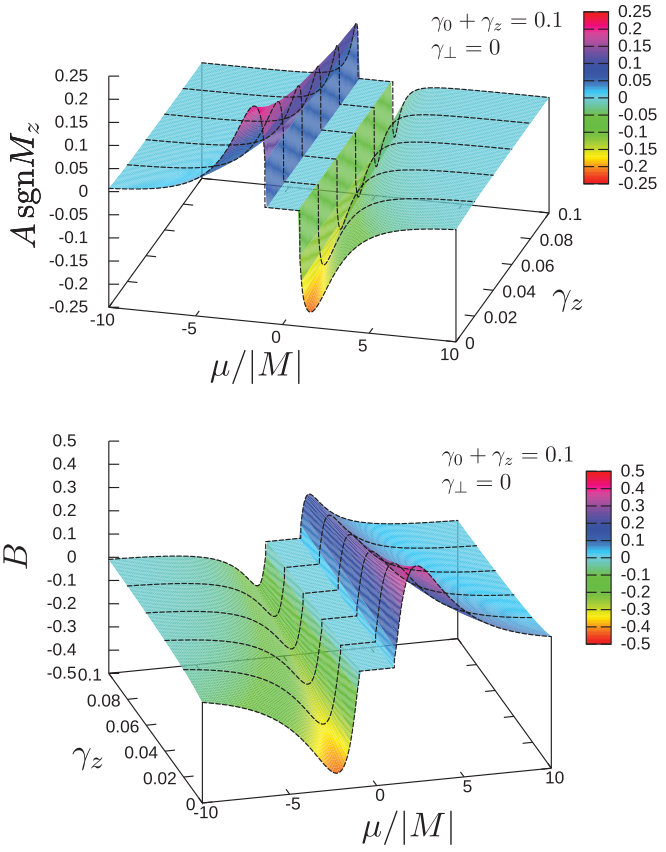

FIG. 10. (Color online) The coefficients A and B of current-induced torques with magnetization gradient as functions of chemical potential μ in the presence of magnetic impurities (γ_z) in addition to normal impurities (γ_0). Their relative magnitudes are changed by keeping $\gamma_0 + \gamma_z = 0.1$ and $\gamma_\perp = 0$.

These features are shared by $\tilde{\alpha}$ and $\delta\tilde{S}$. Relation to transport coefficients will be discussed in the next section.

V. TRANSPORT PICTURE

In the present model, the electron velocity is essentially given by spin $\boldsymbol{v} = v_{\mathrm{F}}(\hat{z} \times \boldsymbol{\sigma})$ [Eq. (3)], and so is the current-density operator

$$\boldsymbol{j} = -ec^\dagger \boldsymbol{v} c = -ev_{\mathrm{F}}\, c^\dagger(\hat{z} \times \boldsymbol{\sigma})c. \tag{74}$$

Because of this relation, various spin properties can be identified with transport properties. In particular, the spin-torque coefficients given by spin-spin response functions $\langle\langle \boldsymbol{\sigma}\,;\,\boldsymbol{\sigma}\rangle\rangle$ (for torques with time derivative) or spin-current response functions $\langle\langle \boldsymbol{\sigma}\,;\,\boldsymbol{j}\rangle\rangle$ (for current-induced torques) can also be expressed as current-current response functions $\langle\langle \boldsymbol{j}\,;\,\boldsymbol{j}\rangle\rangle$, that is, transport coefficients. (Note, however, that this equivalence is actually limited, as will be discussed in Sec. VI D.)

The above equivalence between spin and current also means the equivalence of external perturbations coupled to them. A vector potential $\boldsymbol{A}^{\mathrm{em}}$ (introduced by $\hbar\boldsymbol{k} \to \hbar\boldsymbol{k} + e\boldsymbol{A}^{\mathrm{em}}$) and the exchange field $-M\boldsymbol{u}$ couple to spin $\boldsymbol{\sigma}$ in the combination $-ev_{\mathrm{F}}(\hat{z} \times \boldsymbol{A}^{\mathrm{em}}) - M\boldsymbol{u}$. This means that electrons can not distinguish these two perturbations, and in this sense, they are equivalent. In other words, $\boldsymbol{u}$ contributes to the effective vector potential through

$$\mathcal{A} = \boldsymbol{A}^{\mathrm{em}} - p^{-1}(\hat{z} \times \boldsymbol{u}), \tag{75}$$

or $\boldsymbol{A}^{\mathrm{em}}$ acts as a transverse magnetization through

$$\mathcal{U} = \boldsymbol{u} + p\,(\hat{z} \times \boldsymbol{A}^{\mathrm{em}}), \tag{76}$$

where

$$p = ev_{\mathrm{F}}/M. \tag{77}$$

We now look at some consequences of the above equivalence. First, the coefficients of torques with time derivative are

related to diagonal conductivity (σ_{xx}) and Hall conductivity (σ_{xy}) [53]:

$$\sigma_{xx} = \frac{e^2}{2\pi h}\,\tilde{\alpha}, \quad \sigma_{xy} = \pm\frac{e^2}{2\pi h}\,\delta\tilde{S}. \tag{78}$$

Note that $\mathrm{sgn}(\delta S) = \mathrm{sgn} M$ whereas $\mathrm{sgn}(\sigma_{xy}) = \mathrm{sgn} M_z$. The finite σ_{xy} is due to the anomalous Hall effect. This equivalence has been used in Sec. III to discuss the effects of vertex corrections such as the enhancement of α and δS. Experimental data on the anomalous Hall conductivity in a range of doping level started to be available [63,64].

To the same equivalence class belongs a phenomenon described by $\langle\!\langle \boldsymbol{\sigma}\,;\,\boldsymbol{j}\rangle\!\rangle$. This is the current-induced spin polarization, which has already been presented in Eq. (54), or the resulting spin torque, Eq. (55). This equivalence class is completed by a process expressed by $\langle\!\langle \boldsymbol{j}\,;\boldsymbol{\sigma}\rangle\!\rangle$. This describes a current induced by magnetization dynamics

$$\langle \boldsymbol{j}\rangle = p^{-1}\{\sigma_{xx}\,(\hat{z}\times\dot{\boldsymbol{u}}) + \sigma_{xy}\,\dot{\boldsymbol{u}}\}. \tag{79}$$

This shows that there arises an electromotive force, or an effective electric field,

$$\boldsymbol{E}_{\rm eff} = p^{-1}(\hat{z}\times\dot{\boldsymbol{u}}), \tag{80}$$

due to spin dynamics. This is not a spin-motive force but an electromotive force acting in the charge channel since all electrons feel the same field $\boldsymbol{E}_{\rm eff}$ (same direction) independently of their spin direction.

Another example is the current-induced torques with magnetization gradient [Eq. (59)]. In the transport language, namely, using Eq. (74) and the equivalence of $\boldsymbol{u}$ and $p(\hat{z}\times\boldsymbol{A}^{\rm em})$ [Eq. (76)], it is expressed as [53]

$$\langle \boldsymbol{j}\rangle = \pm ep^2\,\{-A\,\boldsymbol{E} + B\,(\hat{z}\times\boldsymbol{E})\}\,(\mathrm{rot}\boldsymbol{A}^{\rm em})^z. \tag{81}$$

This represents a normal Hall effect due to external magnetic field $(\mathrm{rot}\boldsymbol{A}^{\rm em})^z \equiv H$ applied perpendicularly to the conducting plane. This process gives rise to additional contributions to Eq. (78) by [53]

$$\Delta\sigma_{xx}(H) = \mp ep^2 A\,H, \tag{82}$$

$$\Delta\sigma_{xy}(H) = \mp ep^2 B\,H. \tag{83}$$

Note that the diagonal component σ_{xx} is also modified in the linear order in H. This is because σ_{xy} is nonzero even at $H = 0$ due to the anomalous Hall effect. Note also that these results are gauge invariant with respect to $\boldsymbol{A}^{\rm em}$.

For $|\mu| > |M|$, we observe a relation [53] $B'/\tilde{\alpha}' = \mp A'/\delta\tilde{S}'$ or, equivalently, $\Delta\sigma'_{xy}(H)/\sigma'_{xx} = -\Delta\sigma'_{xx}(H)/\sigma'_{xy}$. This means that, for the case $\gamma_0 \ll 1$, where the single-primed quantities dominate the higher-primed ones, we can define a Hall angle $\theta_{\rm H}$ due to the normal Hall effect by $\tan\theta_{\rm H} = \Delta\sigma_{xy}(H)/\sigma_{xx}$. This is the angle of rotation induced by H in the σ_{xx}-σ_{xy} plane, and is given by

$$\tan\theta_{\rm H} = -\frac{\mu|M|}{\mu^2+M^2}\,\omega_{\rm c}\tau_0 = -\frac{|M|}{\mu}\,\omega_{\rm c}\tau \tag{84}$$

for the case without vertex corrections [65]. Here, $\omega_{\rm c} = eH/m$ is the cyclotron frequency for a nonrelativistic particle with mass $m = |M|/v_{\rm F}^2$, $\tau_0 = \hbar/2\gamma$, and

$$\tau = \frac{\mu^2}{\mu^2+M^2}\,\tau_0 \tag{85}$$

is the lifetime of band electrons at energy μ. At the band edge $\mu \to \pm|M|$, it becomes $\tan\theta_{\rm H} \to \mp\omega_{\rm c}\tau$ as expected, but is suppressed by a factor of $|M|/\mu$ for $|\mu| \gg |M|$. For $|\mu| < |M|$, we observed that $A = B = 0$. This means that the half-quantum value $\sigma_{xy} = \pm e^2/2h$ is not affected by the weak-field normal Hall effect.

Finally, let us consider the conventional current-induced torques, namely, the spin-transfer torque ($\boldsymbol{t} \sim \partial_i\boldsymbol{n}$, where i is the current direction) and the β term ($\boldsymbol{t} \sim \boldsymbol{n}\times\partial_i\boldsymbol{n}$) given by the last two terms in Eq. (9). The absence of these torques is clearly understood in the transport picture, where they are expressed as

$$\langle \boldsymbol{j}\rangle \sim \hat{z}\times\partial_i\boldsymbol{A}^{\rm em}, \quad \partial_i\boldsymbol{A}^{\rm em}. \tag{86}$$

Since these are not gauge invariant, the response coefficients should vanish. Therefore, the spin-transfer torque and the β term are strictly prohibited by the gauge invariance in the present model.

VI. FEEDBACK EFFECTS

Since magnetization dynamics and current flow mutually affect each other, the so-called feedback effects are expected. In this section, we study two such feedback effects. One is the effect of magnetization dynamics on itself via the induced current [32–35], and the other is the effect of current flow on itself via the induced magnetization dynamics.

The former effect was considered for ordinary ferromagnets [32–34] (with no or weak spin-orbit coupling), and recently applied to a ferromagnet with Rashba spin-orbit coupling [35]. Here, we apply it to topological insulator surface states. The latter effect is newly considered in this paper.

A. Feedback torque

First, consider the former effect. A dynamical magnetization $\dot{\boldsymbol{u}}$ induces a current [Eq. (79)] or an effective electric field $\boldsymbol{E}_{\rm eff} = p^{-1}(\hat{z}\times\dot{\boldsymbol{u}})$. The induced current, or the field $\boldsymbol{E}_{\rm eff}$, will exert a torque on the magnetization according to Eq. (55), which may be calculated as [53]

$$\begin{aligned}\Delta\boldsymbol{t}' &= \frac{1}{s_0}\frac{eM}{4\pi^2\hbar v_{\rm F}}\{\delta\tilde{S}\,(\hat{z}\times\boldsymbol{E}_{\rm eff}) \mp \tilde{\alpha}\boldsymbol{E}_{\rm eff}\}\\ &= \mp\alpha_c\,(\hat{z}\times\dot{\boldsymbol{u}}) - \frac{\delta S}{S}\,\dot{\boldsymbol{u}},\end{aligned} \tag{87}$$

with use of Eqs. (7), (8) and (35). As seen, the resulting "feedback torques" are precisely the same as the α_c and δS terms calculated in Sec. III as Eq. (34) without considering the feedback process.

Now, a question arises: Are these "feedback torques" new contributions to be added to the results of Sec. III, or we are just looking at the same thing differently? If the former is the case, α_c and δS will be effectively doubled by the feedback

effect, and the experiments of magnetization dynamics would effectively observe

$$(\alpha_c)_{\rm eff} \stackrel{?}{=} 2\alpha_c, \quad (\delta S)_{\rm eff} \stackrel{?}{=} 2\,\delta S, \tag{88}$$

where α_c and δS on the right-hand sides are the ones calculated in Sec. III. However, in Sec. III, we determined all torques which are first order in $\dot{\boldsymbol{u}}$, namely, such torques are exhausted by Eq. (34). Therefore, what is calculated in Eq. (87) should not be new contributions, not to be added to Eq. (34). Rather, what is done with Eq. (87) is the calculation of Eq. (34) itself in a different way. This means that the feedback process presented here affords a complete physical picture of the Gilbert damping (and spin renormalization) process in this system.

B. Feedback conductivity

Next, consider the latter feedback effect. A current flow, or the driving electric field $\boldsymbol{E}$, induces a torque [Eq. (55)] as expressed by the LLG equation [53]

$$\dot{\boldsymbol{u}} = \pm\frac{1}{s_0 p}\{\sigma_{xy}(\hat{z}\times\boldsymbol{E}) - \sigma_{xx}\boldsymbol{E}\} + \delta\boldsymbol{t}', \tag{89}$$

and the resulting motion of the magnetization $\dot{\boldsymbol{u}}$ induces a current $\Delta\boldsymbol{j}$ according to Eq. (79). Here, $\delta\boldsymbol{t}'$ represents all other torques such as exchange, damping, and magnetic anisotropy. If the effects of $\delta\boldsymbol{t}'$ can be neglected, $\Delta\boldsymbol{j}$ would be obtained as

$$\Delta\boldsymbol{j} = \mp\frac{1}{s_0 p^2}\left\{\left(\sigma_{xx}^2 - \sigma_{xy}^2\right)(\hat{z}\times\boldsymbol{E}) + 2\sigma_{xx}\sigma_{xy}\boldsymbol{E}\right\}. \tag{90}$$

Namely, this effect manifests itself as the change of electrical conductivity $\Delta\sigma_{ij}$. In the above case, one has [53]

$$\Delta\sigma_{xx} = \mp\frac{2a^2}{\hbar S}\left(\frac{M}{e v_{\rm F}}\right)^2 \sigma_{xx}\sigma_{xy}, \tag{91}$$

$$\Delta\sigma_{xy} = \pm\frac{a^2}{\hbar S}\left(\frac{M}{e v_{\rm F}}\right)^2 \left(\sigma_{xx}^2 - \sigma_{xy}^2\right). \tag{92}$$

With [54,55] $v_{\rm F} = 4\times10^5$ m/s, $a = 0.5$ nm, and $S = \frac{1}{2}$, the prefactor is estimated as $(a^2/\hbar S)(M/ev_{\rm F})^2 \sim (10^{-4}$–$10^{-2})h/e^2$ for $M = 0.01$–0.1 eV. If σ_{xy} is comparable to e^2/h or larger, $\Delta\sigma_{xx}/\sigma_{xx}$ may be appreciable. In a metallic regime, $\sigma_{xx} \gg |\sigma_{xy}|$, the ratio $\Delta\sigma_{xy}/\sigma_{xy}$ can be significant.

The above argument [Eqs. (90)–(92)] can be made more realistic if we solve the spin dynamics explicitly by including $\delta\boldsymbol{t}'$. Let us analyze the LLG equation (89) by taking magnetic anisotropy and damping terms in $\delta\boldsymbol{t}'$. (We consider a spatially uniform mode and drop the gradient term.) Suppose we apply an ac electric field $\boldsymbol{E} \propto e^{-i\omega t}$, and induce a ferromagnetic resonance. By solving the linearized LLG equation, and substituting the obtained $\dot{\boldsymbol{u}}$ into Eq. (79), we have [53]

$$\begin{pmatrix}\Delta\sigma_{xx}\\ \Delta\sigma_{xy}\end{pmatrix} = \frac{a^2}{\hbar S_{\rm tot}}\left(\frac{M}{e v_{\rm F}}\right)^2 \frac{\omega}{(\omega_0 - i\alpha\omega)^2 - \omega^2} \times \begin{pmatrix}\pm2\omega\sigma_{xx}\sigma_{xy} + (\alpha\omega + i\omega_0)\left(\sigma_{xx}^2 - \sigma_{xy}^2\right)\\ \mp\omega\left(\sigma_{xx}^2 - \sigma_{xy}^2\right) + 2(\alpha\omega + i\omega_0)\sigma_{xx}\sigma_{xy}\end{pmatrix}, \tag{93}$$

where ω_0 is the resonance frequency (determined by magnetic anisotropy), $S_{\rm tot} = S + \delta S$ is the total spin [Eq. (10)], and $\alpha = (\alpha_d + \alpha_c)S/S_{\rm tot}$ is the total damping constant [Eq. (11)] coming from Eqs. (6) and (34). The feedback corrections $\Delta\sigma_{xx}$ and $\Delta\sigma_{xy}$ of Eq. (93) vanish in the dc limit $\omega \to 0$ since in this case the magnetization just settles into a new equilibrium direction under a static effective field due to current-induced spin. In the high-frequency limit $\omega \gg \omega_0$, they reproduce Eqs. (91) and (92) with corrections due to α. More importantly, they show the frequency dependence reflecting the characteristics of spin dynamics, resonance in this case, and this will enable us an experimental discrimination of this effect. At the resonance frequency, the feedback corrections are enhanced by a factor of α^{-1}, which should be detectable rather easily. This effect can be regarded as an experimental (indirect) measurement of electromotive force generated by magnetization dynamics.

C. Diagrammatic consideration

One may feel uneasy to see the "asymmetry" between the above two feedback effects, namely, while the latter effect (Sec. VI B) provides a new effect, the former (Sec. VI A) does not. To fully understand this, we supplement the argument with Feynman diagrams.

The two feedback effects can be expressed diagrammatically as Figs. 11(a) and 11(b), respectively. Here, for technical simplicity, we have quantized $\boldsymbol{u}$ as magnons, and expressed the magnon propagator by a wavy line. While the vertices $\boldsymbol{\sigma}$ and $\boldsymbol{j}$ are essentially the same (spin-velocity equivalence), there is an obvious difference between the two diagrams: the diagram (b) has a one-particle-reducible magnon line (i.e., it can be disconnected by cutting a single magnon line). It gives

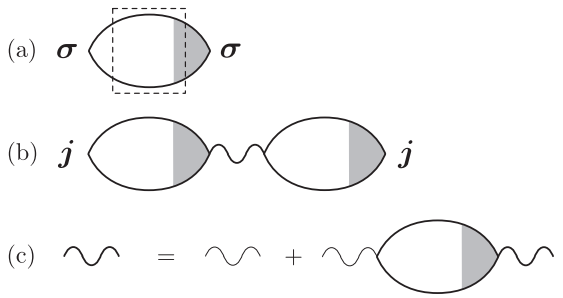

FIG. 11. Diagrammatic expressions for the two feedback effects (a), (b) and the renormalization of magnon propagator (c). (a) The feedback torque due to induced current. This is actually identical to the one calculated in Sec. III. The dashed rectangle indicates the intermediate state discussed in the main text. (b) The feedback correction to conductivity due to induced magnetization dynamics. The wavy line represents the propagator ($\hat{D}$) of induced magnons, and the electron bubble is essentially the conductivity tensor $i\omega\hat{\sigma}$, without feedback effects. (c) Dyson equation for the magnon propagator. The thick (thin) wavy line represents the renormalized (bare) propagator $\hat{D}$ ($\hat{D}_0$). The electron bubble contributes to the self-energy $\hat{\Pi} = M^2\hat{\chi}_\perp = -M^2\hat{\varepsilon}\hat{\sigma}\hat{\varepsilon}/(ev_{\rm F})^2$, which is essentially the transverse spin susceptibility $\hat{\chi}_\perp$, or the (irreducible) conductivity tensor, given by (a).

a correction to the conductivity tensor $(\hat{\sigma})_{ij} = \sigma_{ij}$ by

$$\Delta\hat{\sigma}(\omega) = -\frac{1}{\hbar}\left(\frac{M}{ev_{\rm F}}\right)^2 i\omega\hat{\sigma}\,\hat{\varepsilon}\,\hat{D}(\omega)\hat{\varepsilon}\hat{\sigma}, \tag{94}$$

where $[\hat{D}(\omega)]^{\alpha\beta} = \langle\langle u^\alpha; u^\beta\rangle\rangle_{\omega+i0}$ is the (retarded) Green's function of magnons, and $(\hat{\varepsilon})^{\alpha\beta} = \varepsilon^{\alpha\beta}$ connects the spin and current indices, such that $\boldsymbol{\sigma} = -(ev_{\rm F})^{-1}\hat{\varepsilon}\,\boldsymbol{j}$ [Eq. (74)]. In deriving Eq. (94), we have noted that the two electron bubbles in Fig. 11(b) are given by $\langle\langle \boldsymbol{j}\,;\boldsymbol{\sigma}\rangle\rangle = -(ev_{\rm F})^{-1}\langle\langle \boldsymbol{j}\,;\hat{\varepsilon}\,\boldsymbol{j}\rangle\rangle = +(ev_{\rm F})^{-1}\langle\langle \boldsymbol{j}\,;\boldsymbol{j}\rangle\rangle\hat{\varepsilon}$ and $\langle\langle\boldsymbol{\sigma}\,;\boldsymbol{j}\rangle\rangle = -(ev_{\rm F})^{-1}\hat{\varepsilon}\langle\langle\boldsymbol{j}\,;\boldsymbol{j}\rangle\rangle$, respectively, and that $\langle\langle \boldsymbol{j}\,;\boldsymbol{j}\rangle\rangle = i\omega\hat{\sigma}$. Since $\hat{D}(\omega)$ is calculated as [53,66]

$$\hat{D}(\omega) = \frac{a^2}{S_{\rm tot}}\frac{1}{(\omega_0 - i\alpha\omega)^2 - \omega^2}\begin{pmatrix}\omega_0 - i\alpha\omega & \pm i\omega\\ \mp i\omega & \omega_0 - i\alpha\omega\end{pmatrix}, \tag{95}$$

we see that $\Delta\sigma_{xx}$ and $\Delta\sigma_{xy}$ obtained from Eq. (94) exactly coincide with those in Eq. (93). Such contributions may be called "magnon-drag electrical conductivity."

The magnon propagator used above is the renormalized one in the sense depicted in Fig. 11(c) or expressed by $\hat{D} = \hat{D}_0 + \hat{D}_0\hat{\Pi}\hat{D}$. Here, the bare propagator $\hat{D}_0$ is defined by Eq. (95) with the replacements $\alpha \to \alpha_d$, $S_{\rm tot} \to S$, and $\omega_0 \to \omega_0 S_{\rm tot}/S$ (bare frequency); the difference comes from the magnon self-energy $\hat{\Pi}$ due to the coupling to electrons.

In process (a), the intermediate state, indicated by the dashed rectangle, is a state with an excited spin mode ($\boldsymbol{\sigma}$) by definition, but it can also be viewed as a state with an excited current mode ($\boldsymbol{j}$) because of the spin-velocity equivalence. This fact seems to lie behind the argument of Sec. VI A. There, we have considered the "feedback process" $\boldsymbol{\sigma} \to \boldsymbol{j} \to \boldsymbol{\sigma}$, but this is actually not a sequence of different physical events, but a sequence of different viewpoints on an identical event. Note that all processes in (a) occur within the electron system, while the processes in (b) occur in both electron and magnon systems.

D. Violation of torque-transport correspondence

The results in this section indicate that the equivalence between the torque coefficients and transport coefficients, demonstrated in Sec. V, is actually limited to the case without drag processes. Mathematically, this comes from the fact that these coefficients are not simply defined by the Green's functions [in spite of our (somewhat loose) notation such as $\langle\langle\boldsymbol{\sigma}\,;\boldsymbol{\sigma}\rangle\rangle$], but rather as self-energy parts. The torque coefficients are defined as the self-energy of magnons (or LLG equation), and should be "one-particle irreducible (1PI)" with respect to the magnon propagator. On the other hand, the electrical conductivities are not necessarily 1PI with respect to the magnon propagator. This is why the process shown in Fig. 11(b) is allowed in the conductivity, but not in the torque coefficients.

E. Deviation from the QAH behavior

The results in this section hold also in the QAH state $|\mu| < |M|$. In this case, the magnon-drag contribution leads to the deviation from the QAH behaviors such as the quantization of σ_{xy} and vanishing σ_{xx}.

In the low-frequency limit $\omega \to 0$, Eq. (93) becomes [53]

$$\begin{pmatrix}\Delta\sigma_{xx}\\ \Delta\sigma_{xy}\end{pmatrix} = \frac{e^2}{4\hbar S_{\rm tot}}\left(\frac{a}{\lambda_M}\right)^2\begin{pmatrix}-i\tilde{\omega} + \alpha_d\,\tilde{\omega}^2\\ \pm\tilde{\omega}^2\end{pmatrix}, \tag{96}$$

where $\tilde{\omega} = \omega/\omega_0$. This shows that the quantized value of σ_{xy} at $\omega = 0$ is easily modified by a small ω. (Note that the exact quantization is based on the diagram without drag processes.) Also, the diagonal conductivity becomes finite at finite ω, giving rise to dissipation $\sim\alpha_d\omega^2$. Note that these occur at finite ω but smaller than the gap $|M|$. Since the electron system can not absorb such low energy, the "Joule heating" $\mathrm{Re}(\Delta\sigma_{xx})E^2$ should be ascribed to the dissipation in the magnetization channel; in fact, one can check that the energy dissipation $\alpha_d s_0\dot{\boldsymbol{u}}^2$ (per unit volume) due to the Gilbert damping fully explains the value of the above Joule heating.

At the resonance frequency, $\omega = \omega_0$, which we assume to be smaller than the gap $|M|$, we have $\Delta\sigma_{xx} = \mp i\,\Delta\sigma_{xy} = (e^2/8\hbar S\alpha_d)(a/\lambda_M)^2$, with a small factor α_d in the denominator. With $\alpha_d = 10^{-3}$ and the parameters presented below Eq. (36), this is estimated as $\Delta\sigma_{xx} \sim (10^{-2} \sim 1)(e^2/\hbar)$ for $M = 0.01$–0.1 eV. On the other hand, the quantization of $\delta\tilde{S}$ remains exact since the magnon-drag processes are excluded.

VII. RESULTS AND DISCUSSION

A. Summary of results

So far, we have studied various effects separately. Here, we summarize the results by gathering them in a single place. If we note that $\boldsymbol{u}$ and $\boldsymbol{A}^{\rm em}$ enter in the combination, Eqs. (75) or (76), we may obtain further new terms.

First, the obtained spin torques are summarized as [53]

$$\begin{aligned}\boldsymbol{t}' = {}& \mp\alpha_c\{\hat{z}\times\dot{\boldsymbol{u}} + p\boldsymbol{E}\} - \frac{\delta S}{S}\{\dot{\boldsymbol{u}} - p\,\hat{z}\times\boldsymbol{E}\}\\ & + (e/s_0)\{-A\boldsymbol{E} + B(\hat{z}\times\boldsymbol{E})\}(\mathrm{div}\boldsymbol{u} - pH)\\ & + (e/s_0 p)\{-A(\hat{z}\times\dot{\boldsymbol{u}}) - B\dot{\boldsymbol{u}}\}(\mathrm{div}\boldsymbol{u} - pH).\end{aligned} \tag{97}$$

In the first line, the torques containing $\dot{\boldsymbol{u}}$ are Gilbert damping and spin renormalization, and the torques containing $\boldsymbol{E}$ are due to current-induced (uniform) spin polarization (spin-orbit torque). Those in the second and third lines (with $\mathrm{div}\boldsymbol{u}$) are gradient corrections to them when the magnetization direction is inhomogeneous. The appearance of the external magnetic field H shows that the torques, for example, the Gilbert damping, are linearly affected by the orbital effect.

The magnitudes of these torques are estimated as follows. We use the parameters described in the caption of Table I. (Table I summarizes some results.) We first consider the magnetic-doping case by taking $S = 0.05$. First, from the results of Sec. III, we see

$$\alpha_c \simeq \frac{\pi}{S\gamma_0}\left(\frac{a}{\lambda_M}\right)^2, \quad \left(\frac{\delta S}{S}\right)_{\rm max} \simeq \frac{5}{S}\left(\frac{a}{\lambda_M}\right)^2, \tag{98}$$

where α_c is evaluated at $|\mu| \gg |M|$, and δS is evaluated at the peak (as a function of μ, see Fig. 4). This leads to a large value $\alpha_c \simeq 0.06$. Second, the spin-orbit torques are conveniently estimated by the equivalent magnetic field

$$\gamma_d\boldsymbol{H}_{\rm eff}^{\rm LLG} = \mp\alpha_c p(\hat{z}\times\boldsymbol{E}). \tag{99}$$

TABLE I. Typical magnitudes of several key quantities estimated for $v_F = 4 \times 10^5$ m/s, $a = 0.5$ nm, $M = 0.01$ eV, $\gamma_0 = 0.01$, and $\gamma_d = 1.76 \times 10^{11}$ T^{-1} s^{-1} (free-electron value). The last column shows the dependence on M and γ_0.

Quantity	Value for $M = 0.01$ eV, $\gamma_0 = 0.01$	
$p = ev_F/M$	4×10^9 (cm/V s)	M^{-1}
$\lambda_M = hv_F/M$	1.7×10^{-5} (cm) $= 170$ (nm)	M^{-1}
$(a/\lambda_M)^2$	10^{-5}	M^2
α_c	$0.006 \times (2S)^{-1}$	$M^2\gamma_0^{-1}$
$(\delta S/S)_{\max}$	$10^{-4} \times (2S)^{-1}$	M^2
$H_{\rm eff}^{\rm LLG}$	$0.01S^{-1}$ (T) for $j_{2D} = 0.3$ A/cm	$M\gamma_0^{-1}$
pH	[25 (nm)]$^{-1}$ for $H = 1$ T	M^{-1}

For a moderate current density $j_{3D} = 10^7$ A/cm^2 flowing in a surface region of thickness 0.3 nm (hence the sheet density, $j_{2D} = 0.3$ A/cm), the effective magnetic field is $H_{\rm eff}^{\rm LLG} = 0.2$ T, which is also large. Third, the gradient corrections are smaller by a factor of $\sim 2u\gamma_0 A(\lambda_M/\lambda) \simeq 0.04 \times u \times (\lambda_M/\lambda)$ where λ is the length scale of spatial variation of $\boldsymbol{u}$. This term will be small. This fact, together with the absence of the spin-transfer torque and the β term, indicates that the effects of spatial variation of magnetization are negligible (as far as the magnetization is pointing perpendicularly). Last, the effect of the orbital magnetic field H can be appreciable compared to the equivalent div$\boldsymbol{u}$ term (see the last line of Table I). A field of $H = 1$ T modifies the field-free term, such as α_c (and the spin-orbit torque), by a factor of $\sim$0.27. Since the variation is linear in H, if positive H increases the effective α_c, negative H will decrease it (if the magnetization does not switch). For smaller value of S, all of these effects will be enhanced. On the other hand, for the magnetic-coating case, if we take $S = \frac{1}{2}$, each torque is one order of magnitude smaller than the magnetic-doping case (studied above), which should further be divided by the number of atomic layers (see Sec. II B), and the effects will not be easy to observe.

The results for the electric current density are summarized as [53]

$$\begin{aligned}\langle \boldsymbol{j}\rangle = {}& \sigma_{xx}\left(\boldsymbol{E} + \frac{1}{p}\,\hat{z}\times\dot{\boldsymbol{u}}\right) - \sigma_{xy}\left(\hat{z}\times\boldsymbol{E} - \frac{1}{p}\,\dot{\boldsymbol{u}}\right)\\ & \pm ep\,\{-A\boldsymbol{E} + B(\hat{z}\times\boldsymbol{E})\}\,(pH - \mathrm{div}\boldsymbol{u})\\ & \pm e\,\{-A(\hat{z}\times\dot{\boldsymbol{u}}) - B\dot{\boldsymbol{u}}\}\,(pH - \mathrm{div}\boldsymbol{u})\\ & + \Delta\sigma_{xx}\boldsymbol{E} - \Delta\sigma_{xy}(\hat{z}\times\boldsymbol{E}). \end{aligned} \tag{100}$$

The terms in the first line describe the currents induced by ordinary electric field $\boldsymbol{E}$ and the effective electric field $\boldsymbol{E}_{\rm eff}$ [Eq. (80)] due to spin dynamics. A frequency $\omega = 2\pi \times 100$ MHz of the magnetization dynamics corresponds to the effective electric field $E_{\rm eff} \sim 0.15u$ (V/cm). This is one or two orders of magnitude larger than the Rashba system [22].

The terms in the second and third lines are corrections to those in the first line due to normal Hall effect (H) or magnetization gradient (div$\boldsymbol{u}$). In particular, the magnetization texture with div$\boldsymbol{u} \neq 0$ plays a role of orbital magnetic field on electrons. With the parameters used in the previous section, this effective field is estimated as $H_{\rm eff}^{\rm orb} \sim 25u/\lambda$ T, where λ is measured in nm. These terms (in the first three lines) embody the equivalence of spin torque and electrical transport $\boldsymbol{j} = \mp ps_0\boldsymbol{t}'$.

The last line of Eq. (100) describes the feedback correction or magnon-drag contribution, which violates the above equivalence. Note that the following terms are absent:

$$p^{-1}\{\Delta\sigma_{xx}(\hat{z}\times\dot{\boldsymbol{u}}) + \Delta\sigma_{xy}\dot{\boldsymbol{u}}\}, \tag{101}$$

which might have been expected based on Eq. (75). In other words, the feedback processes do not simply modify σ_{ij} as $\sigma_{ij} + \Delta\sigma_{ij}$ in the first line of Eq. (100). This is because the terms containing $\dot{\boldsymbol{u}}$ in the first line describe electric current induced by a *given* $\dot{\boldsymbol{u}}$, and there is no room for the magnon-drag process to appear. The same reasoning can be applied to the discussion below Eq. (33), and this confirms the statements made in Sec. VI D.

When μ lies in the gap, Eq. (100) becomes

$$\begin{aligned}\langle \boldsymbol{j}\rangle = {}& \frac{e}{4\pi\hbar v_F}\,\mathrm{sgn}M_z\{\dot{\boldsymbol{M}}_\perp - ev_F(\hat{z}\times\boldsymbol{E})\}\\ & + \left(\sigma_0/\omega_0^2\right)\{\omega_0\dot{\boldsymbol{E}} - \alpha_d\ddot{\boldsymbol{E}} \pm (\hat{z}\times\ddot{\boldsymbol{E}})\}, \end{aligned} \tag{102}$$

where $\boldsymbol{M}_\perp = \boldsymbol{M} - M_z\hat{z} = (M_x, M_y, 0)$ with $\boldsymbol{M} = M\boldsymbol{n}$, and $\sigma_0 = (e^2/4\hbar S_{\rm tot})(a/\lambda_M)^2$. The second term in the braces in the first line represents the famous "parity anomaly." The first term was recently used to propose a generation and rectification of electric current due to magnetization precession [67]. The terms in the second line come from the feedback effect, which are estimated in the low-frequency limit, Eq. (96).

B. On the charging of magnetic texture

In Ref. [23], Nomura and Nagaosa proposed a new mechanism (or picture) to electrically drive a domain wall based on their observation that a domain wall (of Néel type) is accompanied by electric charge (for the undoped case). This is equivalent to the mechanism based on the effective magnetic field $M\langle\boldsymbol{\sigma}_\perp\rangle$ due to current-induced spin polarization $\langle\boldsymbol{\sigma}_\perp\rangle$ given by Eq. (54) with $\tilde{\alpha} = 0$. In fact, the effective Lagrangian density $\mathcal{L}' \equiv M\boldsymbol{u}\cdot\langle\boldsymbol{\sigma}_\perp\rangle$, which is written as

$$\mathcal{L}' = \frac{\sigma_{xy}'''}{p}\,\boldsymbol{u}\cdot\boldsymbol{E} = -\frac{\sigma_{xy}'''}{p}\,\boldsymbol{u}\cdot(\nabla\phi^{\rm em} + \dot{\boldsymbol{A}}^{\rm em}), \tag{103}$$

is nothing but (a part of) the Chern-Simons term $\mathcal{L}_{\rm CS} \equiv (\sigma_{xy}'''/2)\varepsilon_{\mu\nu\lambda}\mathcal{A}_\mu\partial_\nu\mathcal{A}_\lambda$. Here, σ_{xy}''' represents the Fermi-sea term as before. On the right-hand side, we have expressed the electric field $\boldsymbol{E}$ by the scalar and vector potentials $\phi^{\rm em}$ and $\boldsymbol{A}^{\rm em}$. A charge accumulation (change of $\rho \equiv -e\langle c^\dagger c\rangle$) induced by magnetization gradient is obtained from $\delta\rho = -\delta\mathcal{L}'/\delta\phi^{\rm em}$ as

$$\delta\rho = \kappa\,\mathrm{div}\boldsymbol{u}, \tag{104}$$

where [53]

$$\kappa = \mp\frac{eM}{4\pi^2\hbar v_F}\,\delta\tilde{S}''' = -\frac{M}{ev_F}\,\sigma_{xy}'''. \tag{105}$$

Note that, in Eq. (104), the combination of ∂_i and u^α is fixed uniquely by gauge invariance. These have been discussed in Refs. [21,23] for the undoped case $|\mu| < |M|$.

We now ask how the above scenario is modified in the doped case $|\mu| > |M|$. In this case, there arise other additional contributions to $\langle\boldsymbol{\sigma}_\perp\rangle$, i.e., the Fermi-surface term $\delta\tilde{S}'$ and the term due to $\tilde{\alpha}$, as expressed by Eq. (54). However, we

found that, in the *static* case $\dot{\boldsymbol{u}} = 0$, to which we restrict ourselves, these terms do not contribute to $\delta\rho$, and Eqs. (104) and (105) continue to hold. As a result, the coefficients of the constituent terms of $\mathcal{L}_{\rm CS}$ become differentiated, and this (apparently) challenges the gauge invariance of $\mathcal{L}_{\rm CS}$. However, the gauge invariance of $\mathcal{L}_{\rm CS}$ is actually intact because of the assumption of *static* situation, where time-dependent gauge transformations are excluded. If we allow time dependence of $\boldsymbol{u}$, the Fermi-surface term $\delta\tilde{S}'$ also contributes to κ. Also, there arises a contribution to $\delta\rho$ due to (spatially inhomogeneous) electromotive force induced by spin dynamics. Deferring the details to elsewhere, here we just comment that, as the driving mechanism of a domain wall, the picture based on the charging of the domain wall seems to be limited to the undoped case, whereas the picture based on the current-induced spin polarization is generally valid including the doped case. We also note that the induced charge, determined by $\delta\tilde{S}'''$, quickly diminishes upon doping as seen from Fig. 4.

VIII. SUMMARY

We have calculated spin torques due to two-dimensional helical electrons as realized on the surface of a topological insulator. We have treated impurity scattering in the (self-consistent) Born approximation for self-energy, and consistently took the ladder-type vertex corrections for response functions. The so-called Fermi-sea terms are also retained.

Thanks to the identity between spin and velocity operators, which is specific to the present model, the obtained spin-torque coefficients have been identified as transport coefficients. This allows us a rather clear understanding of the results such as the effects of vertex corrections.

We have determined all torques up to first orders in $\boldsymbol{u}$, space/time derivative, and electric current. Torques with time derivative are exhausted by Gilbert damping and spin renormalization as usual, and their coefficients are identified as diagonal conductivity and anomalous Hall conductivity. For torques with spatial derivative, ordinary torques (spin-transfer torque and its dissipative correction called β term) have not been obtained. Instead, two new types of current-induced torque are found. The absence of the spin-transfer torque was a surprise since it is the most fundamental spin torque (being based on the angular-momentum conservation), but this fact has been assured by the gauge-invariance argument in the transport picture. We add that we have paid a special care on gauge invariance (Ward-Takahashi identity) in the formulation, which required a careful treatment of ultraviolet divergence. Details of this aspect have been presented in a separate paper [36].

The ordinary current-induced torques (9) will arise if one takes account of some realistic factors beyond the present idealized model, such as deviations of electron dispersion [54,55,68] or the deviation from the current-spin relation (74), but they will remain small compared to ordinary (nontopological) systems.

Finally, we have examined the so-called feedback effects coming from the mutual coupling between spin dynamics ($\dot{\boldsymbol{u}}$) and charge transport ($\boldsymbol{j}$), as expressed by Eqs. (97) and (100). We have shown that the feedback process $\boldsymbol{j} \to \dot{\boldsymbol{u}} \to \boldsymbol{j}$ manifests itself as the modification of electrical conductivity. On the other hand, the process $\dot{\boldsymbol{u}} \to \boldsymbol{j} \to \dot{\boldsymbol{u}}$, which is naively expected to give additional contribution to the Gilbert damping (and spin renormalization), does not actually add a new process but is just a restatement of those obtained by the standard calculation (as done in Sec. III). It, in turn, offers a physical picture of the Gilbert damping in terms of the induced current and its feedback action on the spin dynamics. These contrasting features of the two feedback effects mean the violation of exact correspondence between spin-torque and charge-transport phenomena.

Some of the results of this paper hold also in ferromagnets with Rashba spin-orbit coupling, which will be reported elsewhere.

ACKNOWLEDGMENTS

The authors would like to thank J. Fujimoto, K. Miyake, and Y. Suzuki for valuable discussions. This work was supported by Grants-in-Aid for Scientific Research (Grants No. 21540336, No. 22340104, and No. 24244053) from the Japan Society for the Promotion of Science (JSPS). A.S. is supported by the Global COE Program of JSPS.

APPENDIX A: DETAILS OF CALCULATION

Details of the calculations are presented here. We first consider the processes without vertex corrections in Appendices A 1 and A 2, and then include vertex corrections in Appendix A 3. The velocity renormalization is also considered in Appendix A 3 (but not in Appendices A 1 and A 2). From Appendices A 1 to A 3, only nonmagnetic impurities are considered for simplicity. The effects of magnetic impurities are summarized in Appendix A 4. The topological expression for $\delta\tilde{S}'''$ is derived in Appendix A 5 as Eq. (A99).

1. Gilbert damping and spin renormalization

We study the transverse susceptibility

$$\chi_{\perp}^{\alpha\beta}(i\omega_\lambda) = -T\sum_n \sum_{\boldsymbol{k}} \mathrm{tr}[\sigma^\alpha G_{\boldsymbol{k}}^+ \sigma^\beta G_{\boldsymbol{k}}], \tag{A1}$$

where $\alpha,\beta = x,y$. Writing as $G_{\boldsymbol{k}} = (g_\parallel + g_\perp)D_{\boldsymbol{k}}$ and $G_{\boldsymbol{k}}^+ = (g_\parallel^+ + g_\perp)D_{\boldsymbol{k}}^+$ with

$$g_\parallel = g_0 + g_3\sigma^z, \tag{A2}$$

$$g_\perp = g_1\sigma^x + g_2\sigma^y, \tag{A3}$$

we expand the trace part with respect to $g_\parallel$ and $g_\perp$. Then, the following two terms survive the trace:

$$\mathrm{tr}[\sigma^\alpha g_\parallel^+ \sigma^\beta g_\parallel] = 2(\delta_\perp^{\alpha\beta} X + i\varepsilon^{\alpha\beta} Y), \tag{A4}$$

$$\mathrm{tr}[\sigma^\alpha g_\perp \sigma^\beta g_\perp] = 2(2g_\alpha g_\beta - \delta^{\alpha\beta}\boldsymbol{g}_\perp^2), \tag{A5}$$

where

$$X = X(i\varepsilon_n + i\omega_\lambda, i\varepsilon_n) = g_0^+ g_0 - g_3^+ g_3, \tag{A6}$$

$$Y = Y(i\varepsilon_n + i\omega_\lambda, i\varepsilon_n) = g_0^+ g_3 - g_3^+ g_0. \tag{A7}$$

The term (A5) has d symmetry ($k_x^2 - k_y^2$ or $k_x k_y$) and vanishes after the $\boldsymbol{k}$ integration [69]. Therefore, we have

$$\chi_\perp^{\alpha\beta}(i\omega_\lambda) = -2T\sum_n(\delta_\perp^{\alpha\beta}\varphi + i\varepsilon^{\alpha\beta}\psi), \tag{A8}$$

with

$$\varphi(i\varepsilon_n + i\omega_\lambda, i\varepsilon_n) = X\sum_{\boldsymbol{k}} D_{\boldsymbol{k}}^+ D_{\boldsymbol{k}}, \tag{A9}$$

$$\psi(i\varepsilon_n + i\omega_\lambda, i\varepsilon_n) = Y\sum_{\boldsymbol{k}} D_{\boldsymbol{k}}^+ D_{\boldsymbol{k}}. \tag{A10}$$

After analytic continuation and extracting the ω-linear terms, we have from Eq. (33)

$$\tilde{\alpha} = 4\pi(\hbar v_{\rm F})^2\Big\{\varphi^{(2)}(0,0) - {\rm Re}[\varphi^{(1)}(0,0)] - i\int_{-\infty}^0 d\varepsilon(\partial_\varepsilon - \partial_{\varepsilon'}){\rm Im}[\varphi^{(1)}(\varepsilon,\varepsilon')]|_{\varepsilon'=\varepsilon}\Big\}, \tag{A11}$$

$$\delta\tilde{S} = \pm 4\pi i(\hbar v_{\rm F})^2\Big\{\psi^{(2)}(0,0) - {\rm Re}[\psi^{(1)}(0,0)] - i\int_{-\infty}^0 d\varepsilon(\partial_\varepsilon - \partial_{\varepsilon'}){\rm Im}[\psi^{(1)}(\varepsilon,\varepsilon')]|_{\varepsilon'=\varepsilon}\Big\}. \tag{A12}$$

The Fermi-surface terms are calculated as follows:

$$\varphi^{(2)}(0,0) = X^{\rm RA}I_{011} = \frac{1}{(2\hbar v_{\rm F})^2}\frac{\mu^2+\gamma^2}{2|\mu|\gamma}\frac{\mu^2-M^2}{\mu^2+M^2}C_\zeta, \tag{A13}$$

$$\varphi^{(1)}(0,0) = X^{\rm RR}I_{020} = -\frac{1}{4\pi(\hbar v_{\rm F})^2}, \tag{A14}$$

$$\psi^{(2)}(0,0) = Y^{\rm RA}I_{011} = -\frac{i}{(2\hbar v_{\rm F})^2}\frac{2M_z|\mu|}{\mu^2+M^2}C_\zeta, \tag{A15}$$

and $\psi^{(1)}(0,0) = 0$. We have defined $X^{\rm RA} \equiv X(\varepsilon + i0, \varepsilon - i0)|_{\varepsilon\to 0}$, $X^{\rm RR} \equiv X(\varepsilon + i0, \varepsilon + i0)|_{\varepsilon\to 0}$, and similarly $Y^{\rm RA}$. For the notation $I_{\ell mn}$ and the results of the $\boldsymbol{k}$ integrals, see Appendix B.

The Fermi-sea term $\delta\tilde{S}'''$ [the third term of Eq. (A12)] is calculated as follows:

$$(\partial_\varepsilon - \partial_{\varepsilon'})[\psi^{(1)}(\varepsilon,\varepsilon')]|_{\varepsilon'=\varepsilon} = 2(g_0'g_3 - g_0g_3')\sum_{\boldsymbol{k}}[D_{\boldsymbol{k}}(\varepsilon+i0)]^2 = -\frac{1}{2\pi(\hbar v_{\rm F})^2}\frac{g_0'g_3 - g_0g_3'}{\zeta(\varepsilon)}, \tag{A16}$$

where

$$g_0 \equiv g_0(\varepsilon+i0) = \varepsilon + \mu - \Sigma_0(\varepsilon+i0), \tag{A17}$$

$$g_3 \equiv g_3(\varepsilon+i0) = -M_z + \Sigma_3(\varepsilon+i0), \tag{A18}$$

$$\zeta(\varepsilon) = [\varepsilon + \mu - \Sigma_0(\varepsilon)]^2 - [M_z - \Sigma_3(\varepsilon)]^2, \tag{A19}$$

with $g_i' \equiv \partial g_i/\partial\varepsilon$. By noting $\zeta(\varepsilon) = g_0^2 - g_3^2$, and using $g_0'g_3 - g_0g_3' = (g_0' \pm g_3')g_3 - (g_0 \pm g_3)g_3'$, we have

$$\delta\tilde{S}''' = \pm\,{\rm Im}\int_{-\infty}^0 d\varepsilon\left[\frac{g_0'+g_3'}{g_0+g_3} - \frac{g_0'-g_3'}{g_0-g_3}\right] = \pm\left[{\rm Im}\ln\frac{g_0+g_3}{g_0-g_3}\right]_{-\infty}^0 = \pm\,{\rm Im}\ln\frac{g_0(0)+g_3(0)}{g_0(0)-g_3(0)}. \tag{A20}$$

In the last equality, the contribution from $\varepsilon = -\infty$ drops out since the sign of the imaginary part is the same (positive) between the numerator and the denominator in the logarithm. This expression shows that $\delta\tilde{S}'''$ is determined solely by the quantities at $\varepsilon = 0$ quite generally (e.g., even with self-energy). Explicit evaluation gives

$$\delta\tilde{S}''' = \begin{cases}\pi\,{\rm sgn}M & (|\mu| < |M|),\\ (\varphi_+ - \varphi_-)\,{\rm sgn}M & (|\mu| > |M|),\end{cases} \tag{A21}$$

where

$$\tan\varphi_\pm = \gamma_0\left|\frac{|\mu| \pm |M|}{|\mu| \mp |M|}\right|, \tag{A22}$$

with $0 \leqslant \varphi_\pm \leqslant \pi/2$. As seen, $\delta\tilde{S}'''$ is odd in M and even in μ.

The obtained results are summarized as follows:

(i) For $|\mu| > |M|$,

$$\tilde{\alpha}' = \frac{\pi}{2}\frac{\mu^2+\gamma^2}{\gamma|\mu|}\frac{\mu^2-M^2}{\mu^2+M^2}C_\zeta, \tag{A23}$$

$$\tilde{\alpha}'' = 1, \quad \tilde{\alpha}''' = 0, \tag{A24}$$

$$\delta\tilde{S}' = \frac{2\pi M|\mu|}{\mu^2+M^2}C_\zeta, \quad \delta\tilde{S}'' = 0, \tag{A25}$$

$$\delta\tilde{S}''' = (\varphi_+ - \varphi_-)\,{\rm sgn}M. \tag{A26}$$

(ii) For $|\mu| < |M|$,

$$\tilde{\alpha}' = -1, \quad \tilde{\alpha}'' = 1, \quad \tilde{\alpha}''' = 0, \tag{A27}$$

$$\delta\tilde{S}' = \delta\tilde{S}'' = 0, \quad \delta\tilde{S}''' = \pi\,{\rm sgn}M. \tag{A28}$$

2. Current-induced torques

We next calculate the coefficients of the current-induced torques $K_{ij}^{\alpha\beta}$ shown in Fig. 8(a). By noting $\partial_j G = Gv_jG$ with Eq. (3), we first calculate

$$\tilde{K}_{ij}^{\alpha\beta}(i\omega_\lambda) \equiv T\sum_n\sum_{\boldsymbol{k}}\{{\rm tr}[\sigma^\alpha G_{\boldsymbol{k}}^+\sigma^j G_{\boldsymbol{k}}^+\sigma^\beta G_{\boldsymbol{k}}^+\sigma^i G_{\boldsymbol{k}}] - {\rm tr}[\sigma^\alpha G_{\boldsymbol{k}}^+\sigma^i G_{\boldsymbol{k}}\sigma^\beta G_{\boldsymbol{k}}\sigma^j G_{\boldsymbol{k}}]\} \tag{A29}$$

and then $K_{ij}^{\alpha\beta}$ as

$$K_{ij}^{\alpha\beta} = v_{\rm F}^2\varepsilon_{ii'}\varepsilon_{jj'}\tilde{K}_{i'j'}^{\alpha\beta}. \tag{A30}$$

Using the decomposition $G = (g_\parallel + g_\perp)D$ and $G^+ = (g_\parallel^+ + g_\perp)D^+$, we expand Eq. (A29) with respect to $g_\parallel$ and $g_\perp$. After many cancellations as shown in Figs. 12(b) and 12(c), we are left with terms shown in Fig. 12(a). They are calculated

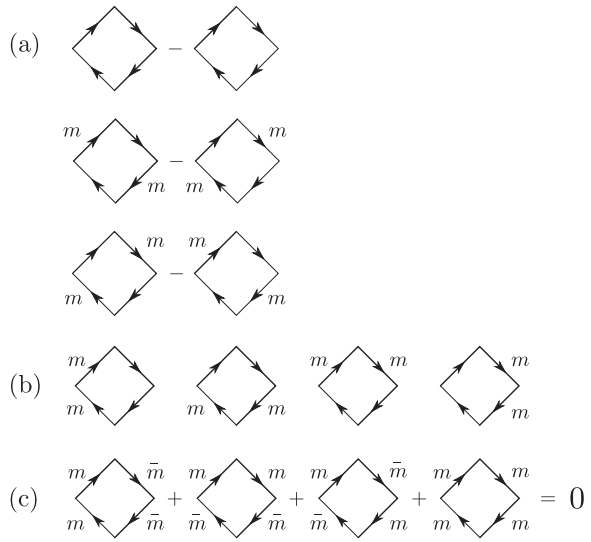

FIG. 12. Contributions to $K_{ij}^{\alpha\beta}$. For simplicity, those without vertex corrections are shown. The original contribution is shown in Fig. 8(a) in which each line represents $G = (g_\parallel + g_\perp)D$. Expansion with respect to $g_\parallel$ and $g_\perp$ generates processes shown in (a)–(c) in this figure. Only (a) contributes to the final result since each diagram of (b) vanishes and the four diagrams of (c) sum to zero. In the figure, a line with a letter m attached represents $g_m\sigma^m$, $m = x, y$, and the one without such a letter represents $g_\parallel$. In (c), $\bar{m} = y$ for $m = x$, and $\bar{m} = x$ for $m = y$. Sum over m is understood. These features remain valid even if the vertex corrections ($\sigma^\alpha \to \Lambda^\alpha$, $v_i \to \tilde{\Lambda}_i$) are included.

as $\tilde{K} = \tilde{K}_1 + \tilde{K}_2 + \tilde{K}_3$ with

$$\tilde{K}_1(i\omega_\lambda) = 2T\sum_n \{X(\delta_\perp^{\alpha i}\delta_\perp^{\beta j} - \varepsilon^{\alpha i}\varepsilon^{\beta j}) + iY(\varepsilon^{\alpha i}\delta_\perp^{\beta j} + \delta_\perp^{\alpha i}\varepsilon^{\beta j})\}(Z^+ J_{031} - Z J_{013}), \tag{A31}$$

$$\tilde{K}_2(i\omega_\lambda) = 2T\sum_n \{X(\delta_\perp^{\alpha i}\delta_\perp^{\beta j} + \varepsilon^{\alpha i}\varepsilon^{\beta j}) + iY(\varepsilon^{\alpha i}\delta_\perp^{\beta j} - \delta_\perp^{\alpha i}\varepsilon^{\beta j})\}(J_{131} - J_{113}), \tag{A32}$$

$$\tilde{K}_3(i\omega_\lambda) = 2T\sum_n (\delta_\perp^{\alpha j}\delta_\perp^{\beta i} + \varepsilon^{\alpha j}\varepsilon^{\beta i})(Z^+ J_{131} - Z J_{113}), \tag{A33}$$

where X and Y are given by Eqs. (A6) and (A7), $Z = g_0^2 - g_3^2$, $Z^+ = (g_0^+)^2 - (g_3^+)^2$, and

$$J_{\ell mn} \equiv \sum_{\boldsymbol{k}} (\hbar\tilde{v}_{\rm F}k)^{2\ell}(D_{\boldsymbol{k}}^+)^m (D_{\boldsymbol{k}})^n. \tag{A34}$$

Here, g_ℓ and D with (without) the superscript "+" have Matsubara frequency $i\varepsilon_n + i\omega_\lambda$ ($i\varepsilon_n$). In deriving the above expressions, we have noted the identities

$$\delta_\perp^{\alpha i}\delta_\perp^{\beta j} - \varepsilon^{\alpha i}\varepsilon^{\beta j} = \delta_\perp^{\alpha j}\delta_\perp^{\beta i} - \varepsilon^{\alpha j}\varepsilon^{\beta i}, \tag{A35}$$

$$\varepsilon^{\alpha i}\delta_\perp^{\beta j} + \delta_\perp^{\alpha i}\varepsilon^{\beta j} = \varepsilon^{\alpha j}\delta_\perp^{\beta i} + \delta_\perp^{\alpha j}\varepsilon^{\beta i}. \tag{A36}$$

After analytic continuation, the ω-linear terms are extracted as $\tilde{K}_\ell(\omega + i0) - \tilde{K}_\ell(0) = (\omega/2\pi)(\tilde{K}'_\ell + \tilde{K}''_\ell + \tilde{K}'''_\ell)$, with the prime notation explained after Eqs. (38) and (39).

From the RA channel, we have

$$\tilde{K}'_1 = 4\{X^{\rm RA}(\delta_\perp^{\alpha i}\delta_\perp^{\beta j} - \varepsilon^{\alpha i}\varepsilon^{\beta j}) + iY^{\rm RA}(\varepsilon^{\alpha i}\delta_\perp^{\beta j} + \delta_\perp^{\alpha i}\varepsilon^{\beta j})\}{\rm Im}(\zeta I_{031}), \tag{A37}$$

$$\tilde{K}'_2 = 4\{X^{\rm RA}(\delta_\perp^{\alpha i}\delta_\perp^{\beta j} + \varepsilon^{\alpha i}\varepsilon^{\beta j}) + iY^{\rm RA}(\varepsilon^{\alpha i}\delta_\perp^{\beta j} - \delta_\perp^{\alpha i}\varepsilon^{\beta j})\}{\rm Im}(I_{131}), \tag{A38}$$

$$\tilde{K}'_3 = 4(\delta_\perp^{\alpha j}\delta_\perp^{\beta i} + \varepsilon^{\alpha j}\varepsilon^{\beta i}){\rm Im}(\zeta I_{131}), \tag{A39}$$

where ζ is given by Eq. (B3), and $I_{\ell mn}$ by Eq. (B1). Using the results of Appendix B, first the relations ${\rm Im}(\zeta I_{031}) = -{\rm Im}(I_{131})$ and ${\rm Im}(\zeta I_{131}) = 0$, and then explicit expressions, we have

$$\tilde{K}'_1 + \tilde{K}'_2 = \frac{\eta}{(\hbar v_{\rm F})^2}\left\{\frac{{\rm Re}\zeta}{\pi|\zeta|^2} + 2|\eta|C_\zeta\right\} \times (X^{\rm RA}\varepsilon^{\alpha i} - iY^{\rm RA}\delta_\perp^{\alpha i})\,\varepsilon^{\beta j} \tag{A40}$$

and $\tilde{K}'_3 = 0$.

From the RR and AA channels, we have $\tilde{K}''_1 = \tilde{K}''_2 = \tilde{K}''_3 = 0$, and

$$\begin{aligned}\tilde{K}'''_1 &= -4(\delta_\perp^{\alpha i}\delta_\perp^{\beta j} - \varepsilon^{\alpha i}\varepsilon^{\beta j}) \times {\rm Im}\int_{-\infty}^0 d\varepsilon\,\zeta(\varepsilon)\,\zeta'(\varepsilon)\,[I_{040}(\varepsilon) - 2\zeta(\varepsilon)I_{050}(\varepsilon)] \\ &= -4(\delta_\perp^{\alpha i}\delta_\perp^{\beta j} - \varepsilon^{\alpha i}\varepsilon^{\beta j}) \times {\rm Im}\int_{-\infty}^0 d\varepsilon\frac{d}{d\varepsilon}\left\{I_{130}(\varepsilon) + \frac{1}{2}I_{020}(\varepsilon) + \frac{1}{2}I_{240}(\varepsilon)\right\},\end{aligned} \tag{A41}$$

$$\begin{aligned}\tilde{K}'''_2 &= -4(\delta_\perp^{\alpha i}\delta_\perp^{\beta j} + \varepsilon^{\alpha i}\varepsilon^{\beta j})\,{\rm Im}\int_{-\infty}^0 d\varepsilon\,\zeta(\varepsilon)\zeta'(\varepsilon)\,[-2I_{150}(\varepsilon)] \\ &= -4(\delta_\perp^{\alpha i}\delta_\perp^{\beta j} + \varepsilon^{\alpha i}\varepsilon^{\beta j}) \times {\rm Im}\int_{-\infty}^0 d\varepsilon\frac{d}{d\varepsilon}\left\{\frac{2}{3}I_{130}(\varepsilon) + \frac{1}{2}I_{240}(\varepsilon)\right\},\end{aligned} \tag{A42}$$

$$\begin{aligned}\tilde{K}'''_3 &= -4(\delta_\perp^{\alpha j}\delta_\perp^{\beta i} + \varepsilon^{\alpha j}\varepsilon^{\beta i}) \times {\rm Im}\int_{-\infty}^0 d\varepsilon\,\zeta'(\varepsilon)\,[I_{140}(\varepsilon) - 2\zeta(\varepsilon)I_{150}(\varepsilon)] \\ &= -4(\delta_\perp^{\alpha j}\delta_\perp^{\beta i} + \varepsilon^{\alpha j}\varepsilon^{\beta i}) \times {\rm Im}\int_{-\infty}^0 d\varepsilon\frac{d}{d\varepsilon}\left\{\frac{1}{3}I_{130}(\varepsilon) + \frac{1}{2}I_{240}(\varepsilon)\right\},\end{aligned} \tag{A43}$$

where $\zeta(\varepsilon)$ is given by Eq. (A19). Note that $\zeta(0) = \zeta$ [Eq. (B3)]. In the above, we have noted the relations $X(\varepsilon + i0, \varepsilon + i0) = \zeta(\varepsilon)$, $D'(\varepsilon) = -D^2(\varepsilon)\zeta'(\varepsilon)$, and thus $I'_{\ell,m-1,0}(\varepsilon) = -(m-1)\zeta'(\varepsilon)I_{\ell m0}(\varepsilon)$, where $' \equiv \partial/\partial\varepsilon$. Using first Eq. (B6) to eliminate all $\zeta(\varepsilon)$'s and then $\zeta'(\varepsilon)I_{\ell m0}(\varepsilon) = -I'_{\ell,m-1,0}(\varepsilon)/(m-1)$ to eliminate $\zeta'(\varepsilon)$, we have expressed the integrands as total derivatives. As a result, the above integrals are given by quantities at $\varepsilon = 0$, namely, by Eq. (B1),

giving

$$\tilde{K}_1''' = \frac{1}{6\pi(\hbar v_F)^2}\,\mathrm{Im}\frac{1}{\zeta}\,(\delta_\perp^{\alpha i}\delta_\perp^{\beta j} - \varepsilon^{\alpha i}\varepsilon^{\beta j}), \tag{A44}$$

$$\tilde{K}_2''' = -\frac{1}{6\pi(\hbar v_F)^2}\,\mathrm{Im}\frac{1}{\zeta}\,(\delta_\perp^{\alpha i}\delta_\perp^{\beta j} + \varepsilon^{\alpha i}\varepsilon^{\beta j}), \tag{A45}$$

and $\tilde{K}_3''' = 0$. Therefore, we obtain

$$\tilde{K}_{ij}^{\alpha\beta} = \frac{\omega}{M^2 v_F^2}(A\delta_\perp^{\alpha i} + B\varepsilon^{\alpha i})\,\varepsilon^{\beta j} \tag{A46}$$

or

$$K_{ij}^{\alpha\beta} = \frac{\omega}{M^2}(A\varepsilon^{i\alpha} + B\delta_\perp^{i\alpha})\,\delta_\perp^{\beta j}. \tag{A47}$$

The coefficients are given by $A = A' + A'' + A'''$ and $B = B' + B'' + B'''$, where

$$A' = -\frac{1}{2\pi^2}\frac{\mu M^2 M_z}{\mu^2 + M^2}\left[\frac{\mu^2(\mu^2 - M^2)(\mu^2 - \gamma^2)}{W} + \frac{\pi|\mu|}{2\gamma(\mu^2 + M^2)}\,C_\zeta\right], \tag{A48}$$

$$B' = \frac{M^2}{8\pi^2}\frac{\mu^2 + \gamma^2}{\mu\gamma}\frac{\mu^2 - M^2}{\mu^2 + M^2}\left[\frac{\mu^2(\mu^2 - M^2)(\mu^2 - \gamma^2)}{W} + \frac{\pi|\mu|}{2\gamma(\mu^2 + M^2)}\,C_\zeta\right], \tag{A49}$$

$$B''' = \frac{M^2}{3\pi^2}\frac{\mu^3\gamma\,(\mu^2 + M^2)}{W}, \tag{A50}$$

and $A'' = A''' = B'' = 0$ with

$$W = (\mu^2 - \gamma^2)^2(\mu^2 - M^2)^2 + (2\mu\gamma)^2(\mu^2 + M^2)^2. \tag{A51}$$

For the undoped case $|\mu| < |M|$, we set $\gamma \to 0$ and obtain [70]

$$A' = B' = B''' = 0. \tag{A52}$$

3. Vertex corrections

Now let us calculate the ladder-type corrections to the σ^α vertex. The σ^α vertex thus renormalized is denoted by Λ^α. We consider several types depending on the analyticity (G^R or G^A) of Green's functions in Λ^α. They satisfy the equation [see Fig. 2(b)]

$$(\Lambda^\alpha)^{CC'} = \sigma^\alpha + n_i u_0^2 \sum_{\boldsymbol{k}} G_{\boldsymbol{k}}^{C}\,(\Lambda^\alpha)^{CC'}\,G_{\boldsymbol{k}}^{C'}, \tag{A53}$$

where $C,C' = A$ or R specifies the analytic branch. Note that Eq. (A53) is written in matrix form, viz., $(G\,\Lambda\,G)_{\sigma\sigma'} = G_{\sigma\sigma_1}\,\Lambda_{\sigma_1\sigma_2}G_{\sigma_2\sigma'}$. The solutions for $\alpha = x,y$ are given in the following:

(i) Case of $|\mu| > |M|$:

$$(\Lambda^\alpha)^{AR} = c_0\,\sigma^\alpha + c_1\,\varepsilon^{\alpha\beta}\sigma^\beta, \tag{A54}$$

$$(\Lambda^\alpha)^{RA} = c_0\,\sigma^\alpha - c_1\,\varepsilon^{\alpha\beta}\sigma^\beta, \tag{A55}$$

$$(\Lambda^\alpha)^{RR} = (\Lambda^\alpha)^{AA} = \xi\,\sigma^\alpha, \tag{A56}$$

where

$$(c_0, c_1) = \frac{(1 - X^{RA}\Pi_0, iY^{RA}\Pi_0)}{(1 - X^{RA}\Pi_0)^2 + (iY^{RA}\Pi_0)^2}, \tag{A57}$$

with $X^{RA} = (1 + \gamma_0^2)(\mu^2 - M^2) \simeq \mu^2 - M^2$, $iY^{RA} = 4\gamma M_z$ [Eqs. (A6) and (A7)],

$$\Pi_0 = n_i u_0^2 \sum_{\boldsymbol{k}} D_{\boldsymbol{k}}^R D_{\boldsymbol{k}}^A = \frac{1 - \chi_\zeta}{2(\mu^2 + M^2)}, \tag{A58}$$

and $\xi = \pi/(\pi + \gamma_0)$ in Eq. (A56) is the same as the velocity renormalization factor (27). Explicitly, they are given by

$$c_0 = \frac{2(\mu^2 + M^2)}{(1 + \chi_\zeta)\mu^2 + (3 - \chi_\zeta)M^2}, \tag{A59}$$

$$c_1 = \frac{8(1 - \chi_\zeta)\gamma M_z(\mu^2 + M^2)}{[(1 + \chi_\zeta)\mu^2 + (3 - \chi_\zeta)M^2]^2}, \tag{A60}$$

where the terms of order γ_0^2 are neglected. If $|\mu|$ is not close to $|M|$, χ_ζ can be dropped. If we write

$$(c_0, c_1) = \rho\,(\cos\theta, \sin\theta), \tag{A61}$$

the effect of the RA-type vertex correction [Eqs. (A54) and (A55)] can be viewed as the dilation (by ρ) and rotation (by θ) in spin space, and that of RR or AA type [Eqs. (A56)] is a simple dilation (by ξ). Together with the velocity renormalization, which multiplies all the torque coefficients by ξ^{-2} [see Eqs. (B4) or (B5)], these effects lead to [53]

$$\tilde{\alpha} = \xi^{-2}\rho\,(\tilde{\alpha}'\cos\theta \mp \delta\tilde{S}'\sin\theta) + \xi^{-1}\tilde{\alpha}'' + \tilde{\alpha}''', \tag{A62}$$

$$\delta\tilde{S} = \xi^{-2}\rho\,(\delta\tilde{S}'\cos\theta \pm \tilde{\alpha}'\sin\theta) + \xi^{-1}\delta\tilde{S}'' + \delta\tilde{S}'''. \tag{A63}$$

$$A = \rho^2\,(A'\cos 2\theta - B'\sin 2\theta) + \xi^2(A'' + A'''), \tag{A64}$$

$$B = \rho^2\,(B'\cos 2\theta + A'\sin 2\theta) + \xi^2(B'' + B'''). \tag{A65}$$

Note that $\delta\tilde{S}'''$ is not renormalized in this procedure because of the cancellation between RR-type vertex corrections and self-energy corrections (velocity renormalization). The results without vertex corrections are obtained by setting $\rho = \xi = 1$ and $\theta = 0$.

So far, the vertex corrections and self-energy themselves have been evaluated with bare velocity. Inclusion of velocity renormalization does not affect the vertex correction in the RA channel (c_0 and c_1) but does affect that in the RR channel (ξ). What is important here, however, is to calculate self-energy and vertex corrections on the same footing, and both yield the same ξ factor. In this sense, we need not pursue this issue further in this paper.

(ii) Case of $|\mu| < |M|$:

The vertex corrections all coincide,

$$(\Lambda^\alpha)^{AR} = (\Lambda^\alpha)^{RA} = (\Lambda^\alpha)^{RR} = (\Lambda^\alpha)^{AA} = \xi\,\sigma^\alpha. \tag{A66}$$

This is natural since there is no distinction between G^R and G^A away from the pole. The torque coefficients are

renormalized as

$$\tilde{\alpha} = \xi^{-1}(\tilde{\alpha}' + \tilde{\alpha}'') + \tilde{\alpha}''', \tag{A67}$$

$$\delta\tilde{S} = \xi^{-1}(\delta\tilde{S}' + \delta\tilde{S}'') + \delta\tilde{S}'''. \tag{A68}$$

$$A = \xi^2(A' + A'' + A'''), \tag{A69}$$

$$B = \xi^2(B' + B'' + B'''), \tag{A70}$$

in general. Actually, only $\delta\tilde{S}'''$ is relevant (other terms vanish), and this is not renormalized because of the cancellation between the velocity renormalization and the vertex correction.

4. Magnetic impurities

In the presence of magnetic impurities, the results so far obtained (and presented in the main text) are modified as follows. As for self-energy, the damping constants are modified to

$$\gamma = \Gamma_1 |\mu| \Theta(\mu^2 - M^2), \tag{A71}$$

$$\gamma' = -\Gamma_2 M_z \Theta(\mu^2 - M^2) \,\mathrm{sgn}\mu, \tag{A72}$$

where

$$\Gamma_1 = \gamma_0 + \gamma_z + 2\gamma_\perp, \tag{A73}$$

$$\Gamma_2 = \gamma_0 + \gamma_z - 2\gamma_\perp, \tag{A74}$$

$$\gamma_z = \frac{n_s u_s^2}{4(\hbar v_F)^2}\overline{S_z^2}, \tag{A75}$$

$$\gamma_\perp = \frac{n_s u_s^2}{4(\hbar v_F)^2}\overline{S_\perp^2}. \tag{A76}$$

[γ_0 is given by Eq. (23) as before.] The velocity renormalization factor (27) is modified to

$$\xi = \frac{\pi}{\pi + (\gamma_0 - \gamma_z)}. \tag{A77}$$

As for vertex corrections, we have Eqs. (A54)–(A56) and (A66) with modified quantities

$$X^{\mathrm{RA}} = \mu^2 - M^2 + \gamma^2 - \gamma'^2, \tag{A78}$$

$$iY^{\mathrm{RA}} = 2\gamma M_z(1 + \Gamma_2/\Gamma_1), \tag{A79}$$

$$\Pi_0 = \frac{\gamma_0 - \gamma_z}{2(\Gamma_1\mu^2 + \Gamma_2 M^2)} C_\zeta, \tag{A80}$$

and ξ given by Eq. (A77). Note that the vertex corrections vanish if $\gamma_z = \gamma_0$.

In the evaluation of $\tilde{\alpha}$, $\delta\tilde{S}$, A, and B, the expressions of the integrals, presented in Appendix B, are not modified if we use Eqs. (A71) and (A72) for γ and γ'. Modification is present only in $\delta\tilde{S}'''$ [Eq. (43)], where $\varphi_\pm$ becomes

$$\varphi_\pm = \tan^{-1}\left|\frac{\Gamma_1|\mu| \pm \Gamma_2|M|}{|\mu| \mp |M|}\right|. \tag{A81}$$

Explicit expressions are as follows. For $|\mu| > |M|$, the results without vertex corrections are given by

$$\tilde{\alpha}' = \frac{\pi}{2}\frac{\mu^2 - M^2}{\Gamma_1\mu^2 + \Gamma_2 M^2}(1 - \chi_\zeta), \tag{A82}$$

$$\tilde{\alpha}'' = 1, \tag{A83}$$

$$\delta\tilde{S}' = \frac{2\pi(\gamma_0 + \gamma_z)M|\mu|}{\Gamma_1\mu^2 + \Gamma_2 M^2}(1 - \chi_\zeta), \tag{A84}$$

$$\delta\tilde{S}''' = \tan^{-1}\left[\frac{4(\gamma_0 + \gamma_z)M|\mu|}{\mu^2 - M^2}\right], \tag{A85}$$

and

$$A' = -\frac{1}{2\pi^2}\frac{(\gamma_0 + \gamma_z)M^2 M_z \mu}{\Gamma_1\mu^2 + \Gamma_2 M^2}\left\{\frac{\mu^2 - M^2}{(\mu^2 - M^2)^2 + 4(\Gamma_1\mu^2 + \Gamma_2 M^2)^2} + \frac{\pi(1 - \chi_\zeta)}{2(\Gamma_1\mu^2 + \Gamma_2 M^2)}\right\}, \tag{A86}$$

$$B' = \frac{1}{8\pi^2}\frac{(\mu^2 - M^2)M^2}{\Gamma_1\mu^2 + \Gamma_2 M^2}\left\{\frac{\mu^2 - M^2}{(\mu^2 - M^2)^2 + 4(\Gamma_1\mu^2 + \Gamma_2 M^2)^2} + \frac{\pi(1 - \chi_\zeta)}{2(\Gamma_1\mu^2 + \Gamma_2 M^2)}\right\}\mathrm{sgn}\mu, \tag{A87}$$

$$B''' = \frac{1}{3\pi^2}\frac{(\Gamma_1\mu^2 + \Gamma_2 M^2)M^2}{(\mu^2 - M^2)^2 + 4(\Gamma_1\mu^2 + \Gamma_2 M^2)^2}\mathrm{sgn}\mu. \tag{A88}$$

If μ is not close to $\pm M$, we have

$$A' \simeq -\frac{1}{4\pi}\frac{(\gamma_0 + \gamma_z)M^2 M_z \mu}{(\Gamma_1\mu^2 + \Gamma_2 M^2)^2}, \tag{A89}$$

$$B' \simeq \frac{1}{16\pi}\frac{(\mu^2 - M^2)M^2}{(\Gamma_1\mu^2 + \Gamma_2 M^2)^2}\mathrm{sgn}\mu, \tag{A90}$$

and $B''' \sim \mathcal{O}(\gamma)$. The vertex corrections are included by using

$$c_0 = 2\frac{\Gamma_1\mu^2 + \Gamma_2 M^2}{\Gamma_1'\mu^2 + \Gamma_2' M^2}, \tag{A91}$$

$$c_1 = \frac{4(\gamma_0^2 - \gamma_z^2)M_z|\mu|}{\Gamma_1'\mu^2 + \Gamma_2' M^2}(1 - \chi_\zeta)c_0, \tag{A92}$$

where

$$\Gamma_1' = (1+\chi_\zeta)\gamma_0 + (3-\chi_\zeta)\gamma_z + 4\gamma_\perp, \tag{A93}$$

$$\Gamma_2' = (3-\chi_\zeta)\gamma_0 + (1+\chi_\zeta)\gamma_z - 4\gamma_\perp. \tag{A94}$$

For $|\mu| < |M|$, the results are the same as the case without magnetic impurities.

5. Topological expression for $\delta\tilde{S}'''$

When μ lies in the gap, $\delta\tilde{S}'''$ has a topological character and takes a quantized value. This is explicitly demonstrated here with self-energy and vertex corrections included. We stress that the consistency between them is necessary to assure this topological character.

From Eq. (A12), it is written as

$$\begin{aligned}\delta\tilde{S}''' &= \mp 2\pi i(\hbar v_{\rm F})^2 \sum_{\boldsymbol{k}} {\rm Im}\int_{-\infty}^{0} d\varepsilon \\ &\quad\times (\partial_\varepsilon - \partial_{\varepsilon'}){\rm tr}[\Lambda^x G(\varepsilon)\Lambda^y G(\varepsilon')]|_{\varepsilon=\varepsilon'} \\ &= \mp 2\pi i\varepsilon_{ij}\sum_{\boldsymbol{k}} {\rm Im}\int_{-\infty}^{0} d\varepsilon \\ &\quad\times {\rm tr}[\,G\,(\partial_\varepsilon G^{-1})G\,(\partial_i G^{-1})G\,(\partial_j G^{-1})],\end{aligned} \tag{A95}$$

where all quantities (Green's function G and vertex function Λ^α) are in the retarded branch $G = G^{\rm R}$, $\Lambda^\alpha = (\Lambda^\alpha)^{\rm RR}$, and "Im" means subtraction of the "advanced" counterpart ($G^{\rm R} \to G^{\rm A}$) followed by division by $2i$. Note that the Ward-Takahashi identity is used in the second equality. An intuitive expression can be obtained by using the form $G = (g_0 + \boldsymbol{g}\cdot\boldsymbol{\sigma})D = g_\mu\sigma^\mu D$ [Eq. (17)]; we first write

$$\delta\tilde{S}''' = \pm 4\pi\varepsilon_{ij}\sum_{\boldsymbol{k}} {\rm Im}\int_{-\infty}^{0} d\varepsilon\, \boldsymbol{d}_0\cdot(\boldsymbol{d}_i\times\boldsymbol{d}_j)[D_{\boldsymbol{k}}(\varepsilon)]^3, \tag{A96}$$

where $\boldsymbol{d}_\mu(\varepsilon) = \boldsymbol{g}\,(\partial_\mu g_0) - g_0(\partial_\mu\boldsymbol{g}) - i(\boldsymbol{g}\times\partial_\mu\boldsymbol{g})$. By defining "normalized" quantities $\hat{\boldsymbol{g}} = \boldsymbol{g}/(\boldsymbol{g}^2)^{1/2}$, $\hat{g}_0 = g_0/(\boldsymbol{g}^2)^{1/2}$, such that $\hat{\boldsymbol{g}}^2 = 1$, we write as $\boldsymbol{d}_\mu(\varepsilon) = \boldsymbol{g}^2\{\hat{\boldsymbol{g}}\,(\partial_\mu\hat{g}_0) - \hat{g}_0(\partial_\mu\hat{\boldsymbol{g}}) - i(\hat{\boldsymbol{g}}\times\partial_\mu\hat{\boldsymbol{g}})\}$. Note that $\hat{\boldsymbol{g}}$ is in general a complex vector because of the self-energy, but the normalization assures that $\partial_\mu\hat{\boldsymbol{g}}$ is orthogonal to $\hat{\boldsymbol{g}}$. After some manipulations, we have

$$\delta\tilde{S}''' = \pm 4\pi\varepsilon_{\mu\nu\lambda}{\rm Im}\sum_{\boldsymbol{k}}\int_{-\infty}^{0} d\varepsilon\,\partial_\mu\left[h_{\boldsymbol{k}}(\varepsilon)\hat{\boldsymbol{g}}\cdot(\partial_\nu\hat{\boldsymbol{g}}\times\partial_\lambda\hat{\boldsymbol{g}})\right], \tag{A97}$$

where $\partial_\mu = \partial/\partial k_\mu$ with $k_\mu = (\varepsilon, k_x, k_y)$. The function $h_{\boldsymbol{k}}(\varepsilon)$ is determined from $\partial_\mu h = (\partial\hat{g}_0/\partial k_\mu)/(\hat{g}_0^2 - 1)^2$ as

$$h_{\boldsymbol{k}}(\varepsilon) = -\frac{\hat{g}_0}{2(\hat{g}_0^2-1)} - \frac{1}{4}\ln\frac{\hat{g}_0-1}{\hat{g}_0+1}. \tag{A98}$$

In deriving Eq. (A97), we have noted that $\varepsilon_{\mu\nu\lambda}\partial_\mu\hat{\boldsymbol{g}}\cdot(\partial_\nu\hat{\boldsymbol{g}}\times\partial_\lambda\hat{\boldsymbol{g}}) = 0$ [71]. Equation (A97) is evaluated as a surface integral; a nonvanishing contribution comes only from the surface $\varepsilon = 0$, where ${\rm Im}h_{\boldsymbol{k}}(0) = -\pi/4$ for $|\mu| < |M|$. (Contributions from other surfaces vanish since $h_{\boldsymbol{k}} = 0$ at $k_\mu = \pm\infty$.) Therefore, we obtain [41]

$$\delta\tilde{S}''' = \mp\frac{1}{2}\int_{-\infty}^{\infty} dk_x\int_{-\infty}^{\infty} dk_y\,\hat{\boldsymbol{g}}\cdot(\partial_x\hat{\boldsymbol{g}}\times\partial_y\hat{\boldsymbol{g}})|_{\varepsilon=0}, \tag{A99}$$

where $\hat{\boldsymbol{g}}\,|_{\varepsilon=0} = (\hbar v_{\rm F}k_y, -\hbar v_{\rm F}k_x, -M_z)/\sqrt{(\hbar v_{\rm F}k)^2 + M^2}$ is a (real) unit vector and defines a map from a two-dimensional (k_x, k_y) plane to a unit sphere $|\hat{\boldsymbol{g}}| = 1$. The integral represents a solid angle swept by $\hat{\boldsymbol{g}}|_{\varepsilon=0}$, giving [53] $-2\pi\,{\rm sgn}M_z = \mp 2\pi\,{\rm sgn}M$, and thus

$$\delta\tilde{S}''' = \pi\,{\rm sgn}M. \tag{A100}$$

APPENDIX B: INTEGRALS

Here, we give a calculation of the integral

$$I_{\ell mn} \equiv \sum_{\boldsymbol{k}} (\hbar\tilde{v}_{\rm F}k)^{2\ell}\left(D_{\boldsymbol{k}}^{\rm R}\right)^m\left(D_{\boldsymbol{k}}^{\rm A}\right)^n, \tag{B1}$$

where $\tilde{v}_{\rm F} = v_{\rm F}$ or $\tilde{v}_{\rm F} = \xi v_{\rm F}$ depending on whether the velocity renormalization [coming from the $\boldsymbol{k}$ dependence of self-energy, see Eqs. (26) and (27)] is considered or not. Let us write as

$$D_{\boldsymbol{k}}^{\rm R} = \frac{1}{\zeta - x}, \quad D_{\boldsymbol{k}}^{\rm A} = \frac{1}{\zeta^* - x}, \tag{B2}$$

with $x = (\hbar\tilde{v}_{\rm F}k)^2$ and

$$\zeta = (\mu + i\gamma)^2 - (M_z + i\gamma')^2. \tag{B3}$$

Then, the integration over $\boldsymbol{k}$ is carried out as

$$\sum_{\boldsymbol{k}} = \frac{2\pi}{(2\pi)^2}\int_0^\infty k\,dk = \frac{1}{4\pi(\hbar\tilde{v}_{\rm F})^2}\int_0^\infty dx, \tag{B4}$$

and thus

$$\begin{aligned} I_{\ell mn} &= \frac{1}{4\pi(\hbar\tilde{v}_{\rm F})^2}\int_0^\infty dx\,\frac{x^\ell}{(\zeta - x)^m(\zeta^* - x)^n} \\ &\equiv \frac{1}{4\pi(\hbar\tilde{v}_{\rm F})^2}\tilde{I}_{\ell mn}. \end{aligned} \tag{B5}$$

The following relations and explicit expressions are easy to verify:

$$\begin{aligned} I_{\ell mn} &= \zeta\, I_{\ell-1,mn} - I_{\ell-1,m-1,n} \\ &= \zeta^* I_{\ell-1,mn} - I_{\ell-1,m,n-1}, \end{aligned} \tag{B6}$$

$$I_{\ell mn} = i\eta\,(I_{\ell m,n-1} - I_{\ell,m-1,n}), \tag{B7}$$

$$\tilde{I}_{0m0} = -\frac{1}{m-1}\frac{1}{\zeta^{m-1}} \quad (m \geqslant 2), \tag{B8}$$

$$\tilde{I}_{011} = \frac{\pi C_\zeta}{|{\rm Im}\,\zeta|} = 2\pi|\eta|\,C_\zeta, \tag{B9}$$

$$\tilde{I}_{021} = -i\frac{\eta}{\zeta} - 2\pi i\eta|\eta|\,C_\zeta, \tag{B10}$$

$$\tilde{I}_{031} = -i\frac{\eta}{2\zeta^2} - \frac{\eta^2}{\zeta} - 2\pi\eta^2|\eta|\,C_\zeta, \tag{B11}$$

where

$$C_\zeta = \begin{cases} 1-\chi_\zeta & (\mathrm{Re}\,\zeta > 0), \\ \chi_\zeta & (\mathrm{Re}\,\zeta < 0), \end{cases} \tag{B12}$$

$$\chi_\zeta = \frac{1}{\pi}\tan^{-1}\frac{|\mathrm{Im}\,\zeta|}{|\mathrm{Re}\,\zeta|}, \tag{B13}$$

$$\eta = \frac{1}{2\,\mathrm{Im}\,\zeta}. \tag{B14}$$

Note that $0 \leqslant \chi_\zeta \leqslant \frac{1}{2}$. These expressions are valid irrespective of the signs of $\mathrm{Re}\,\zeta$ and $\mathrm{Im}\,\zeta$.

Calculation of I_{010} needs special care since it is logarithmically divergent in the ultraviolet. If the loop momentum runs through the impurity potential $u_{\boldsymbol{k}}$, one can interpret and evaluate the integral as

$$n_{\mathrm{i}} u_0^2\, I_{010} \to n_{\mathrm{i}} \sum_{\boldsymbol{k}} |u_{\boldsymbol{k}}|^2 D_{\boldsymbol{k}}^{\mathrm{R}} = \frac{-i\gamma}{\mu + i\gamma}, \tag{B15}$$

where Eqs. (31) and (21) have been used. Otherwise, one needs to introduce additional cutoff such as Λ_{BZ} to make this integral finite. This case happens in the calculation of magnetic anisotropy [72] and the equilibrium polarization $\langle\hat{\sigma}^z\rangle_0$. The gauge invariance assured by the present scheme (based on Λ_{imp}) is intact if $\Lambda_{\mathrm{imp}} < \Lambda_{\mathrm{BZ}}$.

[1] J. C. Slonczewski, J. Magn. Magn. Mater. **159**, L1 (1996).
[2] L. Berger, Phys. Rev. B **54**, 9353 (1996).
[3] S. Zhang and Z. Li, Phys. Rev. Lett. **93**, 127204 (2004).
[4] A. Thiaville, Y. Nakatani, J. Miltat, and Y. Suzuki, Europhys. Lett. **69**, 990 (2005).
[5] X. Waintal and M. Viret, Europhys. Lett. **65**, 427 (2004).
[6] G. Tatara and H. Kohno, Phys. Rev. Lett. **92**, 086601 (2004).
[7] K. Obata and G. Tatara, Phys. Rev. B **77**, 214429 (2008).
[8] A. Manchon and S. Zhang, Phys. Rev. B **78**, 212405 (2008); **79**, 094422 (2009).
[9] I. Miron, G. Gaudin, S. Auffret, B. Rodmacq, A. Schuhl, S. Pizzini, J. Vogel, and P. Gambardella, Nat. Mater. **9**, 230 (2010).
[10] P. Gambardella and I. M. Miron, Philos. Trans. R. Soc. A **369**, 3175 (2011).
[11] K.-W. Kim, S.-M. Seo, J. Ryu, K.-J. Lee, and H.-W. Lee, Phys. Rev. B **85**, 180404 (2012).
[12] D. A. Pesin and A. H. MacDonald, Phys. Rev. B **86**, 014416 (2012).
[13] E. van der Bijl and R. A. Duine, Phys. Rev. B **86**, 094406 (2012).
[14] M. Z. Hasan and C. L. Kane, Rev. Mod. Phys. **82**, 3045 (2010).
[15] J. Moore, Nature (London) **464**, 194 (2010).
[16] X.-L. Qi and S.-C. Zhang, Rev. Mod. Phys. **83**, 1057 (2011).
[17] X.-L. Qi, T. L. Hughes, and S.-C. Zhang, Phys. Rev. B **78**, 195424 (2008).
[18] L. Fu and C. L. Kane, Phys. Rev. Lett. **100**, 096407 (2008).
[19] T. Yokoyama, Y. Tanaka, and N. Nagaosa, Phys. Rev. B **81**, 121401(R) (2010).
[20] S. Mondal, D. Sen, K. Sengupta, and R. Shankar, Phys. Rev. Lett. **104**, 046403 (2010).
[21] I. Garate and M. Franz, Phys. Rev. Lett. **104**, 146802 (2010).
[22] T. Yokoyama, J. Zang, and N. Nagaosa, Phys. Rev. B **81**, 241410 (2010).
[23] K. Nomura and N. Nagaosa, Phys. Rev. B **82**, 161401 (2010).
[24] T. Yokoyama, Phys. Rev. B **84**, 113407 (2011).
[25] W. Luo and X.-L. Qi, Phys. Rev. B **87**, 085431 (2013).
[26] A. Kandala, A. Richardella, D. W. Rench, D. M. Zhang, T. C. Flanagan, and N. Samarth, Appl. Phys. Lett. **103**, 202409 (2013).
[27] S. V. Eremeev, V. N. Men'shov, V. V. Tugushev, P. M. Echenique, and E. V. Chulkov, Phys. Rev. B **88**, 144430 (2013).
[28] Q. Liu, C.-X. Liu, C. Xu, X.-L. Qi, and S.-C. Zhang, Phys. Rev. Lett. **102**, 156603 (2009).
[29] Y. L. Chen, J.-H. Chu, J. G. Analytis, Z. K. Liu, K. Igarashi, H.-H. Kuo, X. L. Qi, S. K. Mo, R. G. Moore, D. H. Lu, M. Hashimoto, T. Sasagawa, S. C. Zhang, I. R. Fisher, Z. Hussain, and Z. X. Shen, Science **329**, 659 (2010).
[30] L. A. Wray, S.-Y. Xu, Y. Xia, D. Hsieh, A. V. Fedorov, Y. S. Hor, R. J. Cava, A. Bansil, H. Lin, and M. Z. Hasan, Nat. Phys. **7**, 32 (2011).
[31] In Eq. (14) of Ref. [22], three terms (including the β term) were obtained for current-induced torques with magnetization gradient. However, they are not gauge invariant in the sense described in Sec. V, so should not be present.
[32] Y. Tserkovnyak, A. Brataas, and G. E. W. Bauer, Phys. Rev. Lett. **88**, 117601 (2002).
[33] Y. Tserkovnyak and C. H. Wong, Phys. Rev. B **79**, 014402 (2009).
[34] S. Zhang and Steven S.-L. Zhang, Phys. Rev. Lett. **102**, 086601 (2009).
[35] K.-W. Kim, J.-H. Moon, K.-J. Lee, and H.-W. Lee, Phys. Rev. Lett. **108**, 217202 (2012).
[36] J. Fujimoto, A. Sakai, and H. Kohno, Phys. Rev. B **87**, 085437 (2013).
[37] See Supplemental Material at http://link.aps.org/supplemental/10.1103/PhysRevB.89.165307 for the list of mathematical symbols.
[38] For example, a clear surface transport measurement has been achieved by using dual gate to remove bulk charge carriers due to unintentional doping in D. Kim, S. Cho, N. P. Butch, P. Syers, K. Kirshenbaum, S. Adam, J. Paglione, and M. S. Fuhrer, Nat. Phys. **8**, 459 (2012).
[39] For a review on topological insulator materials, See Y. Ando, J. Phys. Soc. Jpn. **82**, 102001 (2013).
[40] Y. Tserkovnyak and D. Loss, Phys. Rev. Lett. **108**, 187201 (2012).
[41] D. Culcer, A. H. MacDonald, and Q. Niu, Phys. Rev. B **68**, 045327 (2003); N. A. Sinitsyn, J. E. Hill, H. Min, J. Sinova, and A. H. MacDonald, Phys. Rev. Lett. **97**, 106804 (2006).
[42] S. Raghu, S. B. Chung, X.-L. Qi, and S.-C. Zhang, Phys. Rev. Lett. **104**, 116401 (2010).
[43] H. Kohno and G. Tatara, in *Nanomagnetism and Spintronics*, edited by T. Shinjo (Elsevier, Amsterdam, 2009), Chap. 5.
[44] Y. Tserkovnyak, H. J. Skadsem, A. Brataas, and G. E. W. Bauer, Phys. Rev. B **74**, 144405 (2006).

[45] H. Kohno, G. Tatara, and J. Shibata, J. Phys. Soc. Jpn. **75**, 113706 (2006).

[46] R. A. Duine, A. S. Núñez, J. Sinova, and A. H. MacDonald, Phys. Rev. B **75**, 214420 (2007).

[47] Then, we have to multiply the results by $(M_0/M)^2$, where M_0 and M are unrenormalized and renormalized values of the s-d exchange constant since M in Eqs. (7) and (14) are the bare ones. In this paper, however, we neglect this factor.

[48] Using the density of states $\nu = |\mu|(2\pi\hbar^2 v_{\rm F}^2)^{-1}\Theta(\mu^2 - M^2)$, γ is written as $\gamma = \frac{1}{2}\pi n_{\rm i} u_{\rm i}^2 \nu$. The prefactor $\frac{1}{2}$ is due to the helical nature of electrons since each electron (with a given spin projection) can access only half of the states on the Fermi surface via spin-conserving scatterings. (In other words, ν is for both spin components, whereas γ is for a single spin component.)

[49] In our case, the natural cutoff would be the wave vector at which the surface Dirac band merges and disappears into the bulk-band continuum. This is some fraction of the Brillouin-zone size, hence the notation $\Lambda_{\rm BZ}$ is used.

[50] For example, J. R. Schrieffer, *Theory of Superconductivity* (Benjamin/Cummings, Massachusetts, 1983).

[51] For example, N. H. Shon, and T. Ando, J. Phys. Soc. Jpn. **67**, 2421 (1998).

[52] We use a simplified notation for the linear-response and Matsubara functions

$$\langle\langle \hat{A}; \hat{B}\rangle\rangle_{\omega+i0} = \frac{i}{\hbar}\int_0^\infty dt\, e^{i(\omega+i0)t}\langle[\hat{A}(t), \hat{B}]\rangle,$$

$$\langle\langle \hat{A}; \hat{B}\rangle\rangle_{i\omega_\lambda} = \int_0^{1/T} d\tau\, e^{i\omega_\lambda \tau}\langle \mathrm{T}_\tau \hat{A}(\tau)\hat{B}\rangle,$$

where $\hat{A}$ and $\hat{B}$ are arbitrary operators.

[53] Here, $\pm$ corresponds to $n_z = \pm 1$, and $\mp$ corresponds to $-n_z = \mp 1$; see Eq. (12).

[54] Y. L. Chen, J. G. Analytis, J.-H. Chu, Z. K. Liu, S.-K. Mo, X. L. Qi, H. J. Zhang, D. H. Lu, X. Dai, Z. Fang, S. C. Zhang, I. R. Fisher, Z. Hussain, and Z.-X. Shen, Science **325**, 178 (2009).

[55] D. Hsieh, Y. Xia, D. Qian, L. Wray, J. H. Dil, F. Meier, J. Osterwalder, L. Patthey, J. G. Checkelsky, N. P. Ong, A. V. Fedorov, H. Lin, A. Bansil, D. Grauer, Y. S. Hor, R. J. Cava, and M. Z. Hasan, Nature (London) **460**, 1101 (2009).

[56] N. A. Sinitsyn, A. H. MacDonald, T. Jungwirth, V. K. Dugaev, and J. Sinova, Phys. Rev. B **75**, 045315 (2007).

[57] On the other hand, for $|\mu \pm M| \lesssim \gamma_0|M|$, χ_ζ and $\tan^{-1}(\ldots)$ in Eqs. (43) and (48) can be comparable to unity. However, in this region the present (Born) approximation will not be a good one since the damping is comparable to, or larger than, the Fermi energy.

[58] S. Coleman and B. Hill, Phys. Lett. B **159**, 184 (1985).

[59] If we include only the RA-type vertex corrections but not the RR-type vertex corrections and velocity renormalization (this is done by settting $\xi = 1$), it differs from the curve 1 only slightly (not shown). Therefore, the effect of vertex corrections is mostly determined by the RA-type vertex corrections especially for small γ_0, as is usually the case.

[60] In fact, we have obtained a finite result for δS, but the calculation of $\langle\hat{\sigma}^z\rangle_0$ requires additional cutoff. See the last paragraph in Appendix B.

[61] A. N. Redlich, Phys. Rev. D **29**, 2366 (1984).

[62] For the massless case ($M = 0$), this was shown in T. Fukuzawa, M. Koshino, and T. Ando, J. Phys. Soc. Jpn. **78**, 094714 (2009).

[63] J. G. Checkelsky, J. Ye, Y. Onose, Y. Iwasa, and Y. Tokura, Nat. Phys. **8**, 729 (2012).

[64] C.-Z. Chang, J. Zhang, M. Liu, Z. Zhang, X. Feng, K. Li, L.-L. Wang, X. Chen, X. Dai, Z. Fang, X.-L. Qi, S.-C. Zhang, Y. Wang, K. He, X.-C. Ma, and Q.-K. Xue, Adv. Mater. **25**, 1065 (2013).

[65] When the vertex corrections are included, $\theta_{\rm H}$ is given by

$$\tan\theta_{\rm H} = -\rho\xi^2\frac{\cos(2\theta_{\rm AH} - \theta)}{\cos(\theta_{\rm AH} - \theta)}\frac{|M|}{\mu}\omega_{\rm c}\tau,$$

where $\theta_{\rm AH} = \tan^{-1}(\sigma'_{xy}/\sigma'_{xx})$ is the anomalous Hall angle at $H = 0$. We again see $\tan\theta_{\rm H} \to \pm\omega_{\rm c}\tau$ as $\mu \to \pm|M|$.

[66] The Green's function $\hat{D}(\omega)$ for $\boldsymbol{u}$ can also be obtained by treating $\boldsymbol{u}$ classically based on the LLG equation.

[67] H. T. Ueda, A. Takeuchi, G. Tatara, and T. Yokoyama, Phys. Rev. B **85**, 115110 (2012).

[68] L. Fu, Phys. Rev. Lett. **103**, 266801 (2009).

[69] To make this integral well defined, we need to introduce another cutoff $\Lambda_{\rm BZ}$ which limits the single-particle states to $|\boldsymbol{k}| < \Lambda_{\rm BZ}$, and after dropping terms using the symmetry argument, we let $\Lambda_{\rm BZ} \to \infty$. No modification is necessary in the present regularization scheme (based on $\Lambda_{\rm imp}$) if we keep $\Lambda_{\rm imp} < \Lambda_{\rm BZ}$.

[70] The quantity in the square brackets in Eqs. (A48) and (A49) vanishes like $\sim\gamma^2$.

[71] This fact is usually demonstrated for a real vector by noting that $\partial_\mu\hat{\boldsymbol{g}}$ is orthogonal to $\hat{\boldsymbol{g}}$, and that more than two such vectors are linearly dependent. In the present case, where $\hat{\boldsymbol{g}}$ is a complex vector, it does not enjoy the same reasoning but may be proved as follows: $\varepsilon_{\mu\nu\lambda}\partial_\mu\hat{\boldsymbol{g}}\cdot(\partial_\nu\hat{\boldsymbol{g}}\times\partial_\lambda\hat{\boldsymbol{g}}) = (\boldsymbol{g}^2)^{-5/2}\varepsilon_{\mu\nu\lambda}\{\boldsymbol{g}^2\partial_\mu\boldsymbol{g}\cdot(\partial_\nu\boldsymbol{g}\times\partial_\lambda\boldsymbol{g}) - 3(\boldsymbol{g}\cdot\partial_\mu\boldsymbol{g})\boldsymbol{g}\cdot(\partial_\nu\boldsymbol{g}\times\partial_\lambda\boldsymbol{g})\}$, which vanishes since $\partial_\mu g^\alpha$ vanishes unless $(\mu,\alpha) = (0,z)$, (x,y), or (y,x).

[72] A. S. Núñez and J. Fernández-Rossier, Solid State Commun. **152**, 403 (2012).